EUROPEAN ORGANIZATION FOR NUCLEAR RESEARCH (CERN)

CERN-PH-EP/2013-037
2016/03/07

CMS-EXO-12-041

Search for pair production of first and second generation leptoquarks in proton-proton collisions at $\sqrt{s} = 8\,\text{TeV}$

The CMS Collaboration*

Abstract

A search for pair production of first and second generation leptoquarks is performed in final states containing either two charged leptons and two jets, or one charged lepton, one neutrino and two jets, using proton-proton collision data at $\sqrt{s} = 8$ TeV. The data, corresponding to an integrated luminosity of 19.7 fb^{-1}, were recorded with the CMS detector at the LHC. First-generation scalar leptoquarks with masses less than 1010 (850) GeV are excluded for $\beta = 1.0\ (0.5)$, where β is the branching fraction of a leptoquark decaying to a charged lepton and a quark. Similarly, second-generation scalar leptoquarks with masses less than 1080 (760) GeV are excluded for $\beta = 1.0\ (0.5)$. Mass limits are also set for vector leptoquark production scenarios with anomalous vector couplings, and for R-parity violating supersymmetric scenarios of top squark pair production resulting in similar final-state signatures. These are the most stringent limits placed on the masses of vector leptoquarks and RPV top squarks to date.

Published in Physical Review D as doi:10.1103/PhysRevD.93.032004.

*See Appendix A for the list of collaboration members

1 Introduction

The structure of the standard model (SM) of particle physics exhibits a symmetry between quarks and leptons. This paper reports on a search with the CMS detector at the CERN LHC for leptoquark (LQ) particles. These particles, which manifest a fundamental connection between quarks and leptons, are hypothesized by a variety of extensions to the SM such as grand unified theories [1–8], extended technicolor models [9–11], superstring-inspired models [12], and composite models with lepton and quark substructure [13]. Leptoquarks carry both baryon (B) and lepton (L) quantum numbers and thus couple to leptons and quarks. They carry fractional electric charge, are color triplets under $SU(3)_C$, and can be either scalar or vector particles. Other properties such as their weak isospin, the helicity of the quarks and leptons to which they couple, and their fermion number $F = (3B + L)$ depend on the specific structure of each model. Interpretations of direct searches for LQs at particle colliders rely on effective theories, such as the one described in Ref. [14], which require LQs to have renormalizable interactions, to obey SM gauge group symmetries, and to couple only to SM fermions and gauge bosons. In order to ensure proton stability, in effective theories LQs are generally constrained to conserve lepton and baryon numbers separately. Moreover, existing experimental limits [15, 16] on lepton number violation, flavor changing neutral currents, and other rare processes favor three generations of LQs with no intergenerational mixing, which is the scenario considered here.

A search for pair production of first and second generation leptoquarks is performed in final states containing either two charged leptons and two jets, or one charged lepton, one neutrino and two jets, using proton-proton collision data at $\sqrt{s} = 8$ TeV. The data, corresponding to an integrated luminosity of 19.7 fb^{-1}, were recorded with the CMS detector at the LHC. At hadron colliders, LQs would be produced in pairs or singly; this paper concentrates on LQ pair production. Recent CMS results for single LQ production are documented in Ref. [17].

The production and decay of a scalar LQ are characterized by its mass (M_{LQ}), its decay branching fraction β into a charged lepton and a quark, and the Yukawa coupling $\lambda_{\ell q}$ characterizing the LQ-lepton-quark vertex. The interaction of scalar LQs with SM bosons is completely determined by these three parameters [14]. The interaction of vector LQs with the SM bosons additionally depends on two anomalous couplings λ_G and κ_G, which relate to the anomalous magnetic and electric quadrupole moments of the LQ that can be present in the $\text{gLQ}\overline{\text{LQ}}$ and $\text{ggLQ}\overline{\text{LQ}}$ vertices [18], where g represents a gluon and $\overline{\text{LQ}}$ represents the anti-LQ. Four scenarios for the values of the anomalous couplings are typically considered in this case: minimal couplings (MC), $\lambda_G = 0$, $\kappa_G = 1$; Yang–Mills (YM) type couplings, $\lambda_G = \kappa_G = 0$; minimal-minimal (MM) couplings, $\lambda_G = \kappa_G = -1$; and the case of absolute minimal (AM) cross section with respect to the λ_G, κ_G parameters for each value of LQ mass.

LQ pair production arises predominantly through gluon-gluon fusion and quark-antiquark annihilation, shown in Fig. 1, which have been calculated using next-to-leading order (NLO) QCD corrections [19]. The dominant pair production mechanisms for scalar LQs do not depend on $\lambda_{\ell q}$ and the search sensitivity can be considered $\lambda_{\ell q}$-independent as long as $\lambda_{\ell q}$ is sufficiently large so that LQs decay within a few mm of the primary vertex.

Other scenarios of physics beyond the SM could also lead to the prediction of particles with LQ-type couplings. One such theory is supersymmetry (SUSY), which postulates a symmetry between fermions and bosons, and predicts in some models the existence of quark superpartners (squarks), such as the top quark superpartner (top squark, $\tilde{\text{t}}$), decaying into LQ-like final states if R-parity is violated (RPV) [20]. We consider one such model [21], where top squark decay is mediated by a Higgsino ($\tilde{\text{H}}$) with a mass $M_{\tilde{\text{H}}} = M_{\tilde{\text{t}}} - 100\,\text{GeV}$ with a 100% branching fraction. The Higgsino in turn produces an off-shell top squark, which decays to a charged

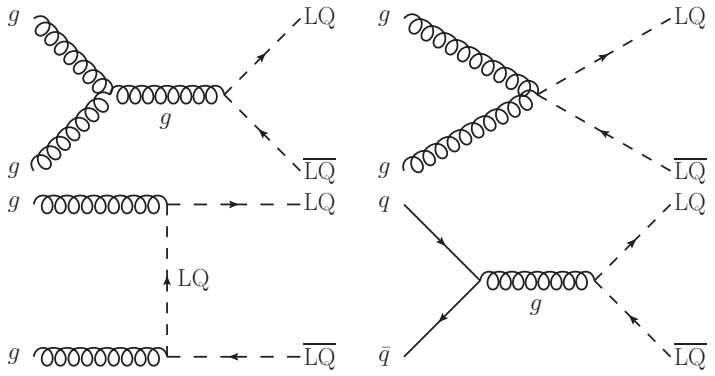

Figure 1: Dominant leading order diagrams for the pair production of scalar leptoquarks.

lepton and a quark, as shown in Fig. 2. The top squark decays via the RPV λ'_{ijk} vertex, where λ'_{ijk} represents the Yukawa coupling of the RPV term of the superpotential, and the ijk indices represent the family numbers of the interaction superfields, which correspond to λ'_{132} for the electron final state and λ'_{232} for the muon final state. Limits have not previously been set on this model.

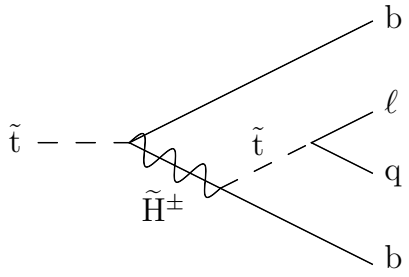

Figure 2: Diagram of the Higgsino-mediated top squark decay via the RPV λ'_{132} (ℓ=e) or λ'_{232} (ℓ=μ) coupling.

The final-state event signatures of the decay of pair-produced LQs can be classified as: dilepton and jets (both LQ and $\overline{\text{LQ}}$ decay into a charged lepton and a quark); single lepton, missing transverse momentum and jets (one LQ decays into a charged lepton and a quark, while the other decays into a neutrino and a quark); and missing transverse momentum and jets (both LQ and $\overline{\text{LQ}}$ decay into neutrinos and quarks). The three signatures correspond to branching fractions of β^2, $2\beta(1-\beta)$, and $(1-\beta)^2$, respectively. The charged leptons can be either electrons, muons, or tau leptons, corresponding to the three generations of LQs. Only final states containing electrons and muons are considered here, and two distinct signatures: one with two high transverse momentum (p_{T}) charged leptons and two high p_{T} jets (denoted as $\ell\ell$jj), and the other with one high p_{T} charged lepton, large missing transverse momentum, and two high p_{T} jets (denoted as $\ell\nu$jj). These final states are analyzed in the context of scalar LQs, vector LQs [22] and the RPV SUSY scenario previously mentioned.

The most stringent limits on the pair-production of scalar LQs come from the LHC experiments. The ATLAS experiment excluded first (second) generation LQs with masses below 1050 (1000) GeV for $\beta = 1$, and 900 (850) GeV for $\beta = 0.5$, using 20 fb^{-1} of $\sqrt{s} = 8$ TeV data [23]. Using $\sqrt{s} = 7$ TeV proton-proton collisions data corresponding to an integrated luminosity of 5.0 fb^{-1}, the CMS experiment excluded first- (second-)generation pair-produced scalar LQs

with masses below 830 (840) GeV for $\beta = 1$ and 640 (650) GeV for $\beta = 0.5$ [24]. CMS excluded third-generation pair-produced scalar LQs with masses below 740 GeV for $\beta = 1$, using 19.7 fb^{-1} of $\sqrt{s} = 8$ TeV data [25]. ATLAS excluded third-generation pair-produced scalar LQs with masses below 534 GeV for $\beta = 1$, using 4.7 fb^{-1} of $\sqrt{s} = 7$ TeV data [26]. The HERA experiments H1 [27] and ZEUS [28] produced λ-dependent results for LQ models, excluding scalar LQ masses up to roughly 500–650 (300) GeV for $\lambda = 1.0$ (0.3). Searches for scalar LQs have also been performed by the Tevatron experiments D0 [29–31] and CDF [32–34]. The most stringent limits on vector LQs have been reported by D0 [35–37] and CDF [38].

2 The CMS detector

The central feature of the CMS apparatus is a superconducting solenoid of 6 m internal diameter, providing a magnetic field of 3.8 T. Within the solenoid volume are a silicon pixel and strip tracker, a lead tungstate crystal electromagnetic calorimeter (ECAL), and a brass and scintillator hadron calorimeter (HCAL), each composed of a barrel and two endcap sections. Muons are measured in gas-ionization detectors embedded in the steel flux-return yoke outside the solenoid. Extensive forward calorimetry complements the coverage provided by the barrel and endcap detectors. A more detailed description of the CMS detector, together with a definition of the coordinate system used and the relevant kinematic variables, can be found in Ref. [39].

The inner tracking system of CMS consists of a silicon pixel and strip tracker, providing the required granularity and precision for the reconstruction of vertices of charged particles in the range of the azimuthal angle $0 \leq \phi < 2\pi$ and pseudorapidity $|\eta| < 2.5$. The crystal ECAL and the brass and scintillator sampling HCAL are used to measure the energies of photons, electrons, and hadrons within $|\eta| < 3.0$. The electron momentum is estimated by combining the energy measurement in the ECAL with the momentum measurement in the tracker. The momentum resolution for electrons with $p_T \approx 45$ GeV from $Z \to ee$ decays ranges from 1.7% for nonshowering electrons in the barrel region to 4.5% for showering electrons in the endcaps [40].

The CMS detector is nearly hermetic, which allows for a measurement of missing transverse momentum. The three muon systems surrounding the solenoid cover the region $|\eta| < 2.4$ and are composed of drift tubes in the barrel region ($|\eta| < 1.2$), cathode strip chambers in the endcaps ($0.9 < |\eta| < 2.4$), and resistive-plate chambers in both the barrel region and the endcaps ($|\eta| < 1.6$). Events are recorded based on a trigger decision using information from the CMS detector subsystems. The first level (L1) of the CMS trigger system, composed of custom hardware processors, uses information from the calorimeters and muon detectors to select the most interesting events in a fixed time interval of less than 4 μs. The high-level trigger (HLT) processor reduces the event rate from 100 kHz at L1 to roughly 400 Hz.

3 Data and simulation samples

The data used in this paper correspond to an integrated luminosity of (19.7 ± 0.5) fb^{-1}. The integrated luminosity is measured as described in Ref. [41].

For the searches in the eejj and eνjj channels, events are selected by triggers requiring at least one electron with $p_T > 30$ GeV, at least one jet with $p_T > 100$ GeV, and at least one additional jet with $p_T > 25$ GeV. For the determination of the hadronic multijet background in the eejj and the eνjj channels, events are selected using single-photon triggers, which require at least one ECAL energy deposit.

Events in the $\mu\mu$jj and the $\mu\nu$jj channels are selected if they pass a single-muon trigger selection that requires a muon with $p_T > 40$ GeV, $|\eta| < 2.1$. There are no isolation requirements. This selection is also used to provide a sample of eμjj events for the determination of the $t\bar{t}$ background in both $\ell\ell$jj channels.

Simulated signal and background samples are produced and fully reconstructed using a simulation of the CMS detector based on GEANT4 [42]. These simulations include additional collisions in a single bunch crossing (pileup) with a distribution matched to the number of pileup events observed during the various data-taking periods.

Signal samples for scalar LQ masses from 300 to 1200 GeV in 50 GeV steps were generated at the leading-order (LO) level with the PYTHIA event generator [43] and CTEQ6L1 [44] parton distribution function (PDF) set. These samples are used to study the acceptance, while NLO cross sections are used for comparison in the limit-setting procedure. With the exception of the RPV SUSY sample described below, PYTHIA 6.422 with the Z2 tune [45] was used. The search limits being $\lambda_{\ell q}$-independent, these samples were generated with a coupling strength $\lambda_{\ell q} = 0.3$. The vector LQ signal samples were generated with the CALCHEP version 3.4 event generator [46] and CTEQ6L PDF set using the model with vector LQ implemented in Ref. [22]. Vector LQ masses between 200 and 1800 GeV were generated in 100 GeV steps, for the four scenarios of the anomalous couplings λ_G and κ_G described in Section 1. Samples of RPV SUSY events were produced with eejj and $\mu\mu$jj final state signatures. These samples were produced for top squark masses from 300 to 1000 GeV in 50 GeV steps using PYTHIA 8.175 [47] and their decays were simulated withd MADGRAPH 5.1.1 [48]. Top squark production cross sections were calculated at the NLO + next-to-leading-logarithm (NLL) level using PROSPINO [49] and the NLL-FAST program [50, 51], using the CTEQ6M PDF set.

The main sources of background for these searches are $t\bar{t}$, single top quark, Z/γ^*+jets, W+jets, diboson (ZZ/WZ/WW)+jets, and multijet production. Backgrounds in the $\ell\ell$jj channels from multijet production and $t\bar{t}$ events are estimated from data control regions, while single top quark, Z/γ^*+jets, W+jets, and diboson (ZZ/WZ/WW)+jets backgrounds are estimated using simulated events. In the $\ell\nu$jj channel, the $t\bar{t}$ background is also estimated using simulated events. The simulated samples of $t\bar{t}$, Z/γ^*+jets, and W+jets are generated with MADGRAPH; single top quark samples (s-, t-, and tW- channels) are generated with POWHEG version 1.0 [52–55]; and samples of VV, where V represents either a W or Z boson, are generated with PYTHIA. The simulations with MADGRAPH and PYTHIA use the CTEQ6L1 PDF set. The simulations with POWHEG use the CTEQ6M PDF set.

The W+jets and Z/γ^*+jets samples are normalized to next-to-NLO (NNLO) inclusive cross sections calculated with FEWZ version 3.1 [56]. Single top quark and VV samples are normalized to NLO inclusive cross sections calculated with MCFM version 6.6 [57–60]. Results from Refs. [61, 62] are used to normalize the $t\bar{t}$ sample at the NNLO + next-to-NLL level.

4 Event reconstruction and selection

Electron candidates are created by matching an electromagnetic cluster in the ECAL in η and ϕ to a reconstructed track in the inner tracking system. The ECAL cluster must have a shower shape and longitudinal profile consistent with that of an electromagnetic shower. The matching reconstructed track can lack a hit in at most one pixel layer, and must be within 0.02 (0.05) cm of the matched primary vertex in the barrel (endcap). The resulting electron candidates are required to pass a set of criteria optimized for electrons with energies of hundreds of GeV [40]. In particular, they must have transverse momenta $p_T > 35$ GeV and $|\eta| < 2.5$, excluding the

transition region between the barrel and endcap detectors, $1.442 < |\eta| < 1.560$, where the electron reconstruction is suboptimal. The transverse momentum sum of tracks in a cone of $\Delta R = \sqrt{(\Delta\phi)^2 + (\Delta\eta)^2} = 0.5$ around the electron candidate's track must be less than 5 GeV, which reduces the chance of jets being misidentified as electrons. Tracks used in this momentum sum, known as tracker isolation, must be within 0.2 cm of the z coordinate of the electron candidate's matching primary vertex to eliminate tracks coming from other proton-proton collisions in the same bunch crossing. The transverse energy sum of the calorimeter energy deposits falling in the $\Delta R = 0.5$ cone is required to be less than about 3% of the candidate's transverse energy. This energy sum, known as calorimeter isolation, has an extra contribution accounting for the average contribution of additional proton-proton collisions in the same bunch crossing.

Muons are reconstructed as tracks combining hit segments in the muon system and hits in the inner tracking system [63]. Muons are required to have $p_T > 45$ GeV and to be contained in the fiducial volume used for the HLT muon selection, $|\eta| < 2.1$. In addition, muons are required to satisfy a set of identification criteria optimized for high p_T. They require at least one muon detector segment be included in the muon track fit, and segments in at least two muon stations be geometrically matched to a track in the inner tracking system. Isolated muons are selected by requiring that the sum of the transverse momenta of all tracks in the tracker in a cone of $\Delta R = 0.3$ around the muon track (excluding the muon track itself), divided by the muon p_T, is less than 0.1. To have a precise p_T measurement and to suppress muons from decays in flight, at least 8 tracker layers with associated hits are required, and at least one hit in the pixel detector. To reject muons from cosmic rays, the transverse impact parameter with respect to the primary vertex is required to be less than 2 mm and the longitudinal distance of the tracker-only track with respect to the primary vertex is required to be less than 5 mm, where the primary vertex is defined as the reconstructed vertex for which the p_T^2 sum of the assigned tracks is largest [64].

Events are reconstructed using a particle-flow (PF) algorithm [65, 66], which identifies and measures stable particles by combining information from all CMS sub-detectors. The missing transverse momentum vector $\vec{p}_T^{\,\text{miss}}$ is defined as the projection on the plane transverse to the beams of the negative vector of the momenta of all particles reconstructed with the PF algorithm in the event, and the missing transverse energy (E_T^{miss}) is defined as the magnitude of the $\vec{p}_T^{\,\text{miss}}$ vector. Jets are reconstructed using the anti-k_T [67, 68] algorithm with a distance parameter of 0.5. The jet energy is calibrated using the p_T balance of dijet and γ+jet events in both data and simulation [69]. The PF jet energy resolution is 15% at 10 GeV, 8% at 100 GeV, and 4% at 1 TeV, to be compared to about 40%, 12%, and 5% obtained when the calorimeters alone are used for jet clustering. The leading (sub-leading) jet is required to have $p_T > 125$ (45) GeV. All jets are required to have $|\eta| < 2.4$. Furthermore, only jets having a spatial separation from electron or muon candidates of $\Delta R > 0.3$ are considered.

4.1 The $\ell\ell$jj channel

An initial selection is made to obtain events containing at least two charged lepton candidates (either two electrons or two muons) and at least two jets for this channel. The two highest p_T leptons and the two highest p_T jets are considered as the decay products from a pair of LQs. They must satisfy the identification criteria described above. Further, the invariant mass of the two leptons, $M_{\ell\ell}$, is required to be larger than 50 GeV. Muons are required to be spatially separated from one another by $\Delta R > 0.3$. The scalar sum of the transverse momenta of the selected final state leptons and jets in the event $S_T = p_T(\ell_1) + p_T(\ell_2) + p_T(j_1) + p_T(j_2)$ is required to be larger than 300 GeV. No charge requirement is placed on the leptons. After this initial selection, the signal-to-background separation is optimized by maximizing $S/\sqrt{S+B}$, where S and B represent numbers of signal and background events, respectively. This is done by varying

cuts on certain kinematic variables, and selecting the combination of cuts with the maximum $S/\sqrt{S+B}$. Three variables are optimized for each LQ mass hypothesis in both $\ell\ell$jj channels: S_{T}; $M_{\ell\ell}$, used to remove most of the contribution from the Z/γ^*+jets background; and $M^{\mathrm{min}}_{\ell,\mathrm{jet}}$, defined as the smaller of the two lepton-jet invariant masses, given the combination that minimizes the $\mathrm{LQ} - \overline{\mathrm{LQ}}$ invariant mass difference.

The eejj and $\mu\mu$jj channels are optimized separately and the optimized thresholds are summarized in Tables 1 and 2, respectively. For the mass hypotheses beyond 1 TeV the same set of final selections as those for the 1 TeV mass hypothesis is used.

Table 1: Optimized thresholds for different LQ mass hypotheses of the eejj signal.

	LQ mass [GeV]														
	300	350	400	450	500	550	600	650	700	750	800	850	900	950	≥ 1000
S_{T} [GeV]	435	485	535	595	650	715	780	850	920	1000	1075	1160	1245	1330	1425
M_{ee} [GeV]	110	110	115	125	130	140	145	155	160	170	175	180	190	195	205
$M^{\mathrm{min}}_{\mathrm{ej}}$ [GeV]	50	105	160	205	250	290	325	360	390	415	435	450	465	470	475

Table 2: Optimized thresholds for different LQ mass hypotheses of the $\mu\mu$jj signal.

	LQ mass [GeV]														
	300	350	400	450	500	550	600	650	700	750	800	850	900	950	≥ 1000
S_{T} [GeV]	380	460	540	615	685	755	820	880	935	990	1040	1090	1135	1175	1210
$M_{\mu\mu}$ [GeV]	100	115	125	140	150	165	175	185	195	205	215	220	230	235	245
$M^{\mathrm{min}}_{\mu\mathrm{j}}$ [GeV]	115	115	120	135	155	180	210	250	295	345	400	465	535	610	690

4.2 The $\ell\nu$jj channel

Events in this channel are selected to contain exactly one charged lepton (electron or muon), at least two jets, and $E^{\mathrm{miss}}_{\mathrm{T}} > 55\,\mathrm{GeV}$. Leptons and jets must meet the criteria described above. Events containing a second lepton (electron or muon) are vetoed for the $\ell\nu$jj selections. In addition, in order to reject events with mis-reconstructed $E^{\mathrm{miss}}_{\mathrm{T}}$, the angle in the transverse plane between the direction of the leading p_{T} jet and the $\vec{p}^{\,\mathrm{miss}}_{\mathrm{T}}$ vector, $\Delta\phi(\vec{p}^{\,\mathrm{miss}}_{\mathrm{T}}, \mathrm{j}_1)$ is required to be larger than 0.5. For the same reason, the electron or muon and the $\vec{p}^{\,\mathrm{miss}}_{\mathrm{T}}$ are required to be separated by $\Delta\phi(\vec{p}^{\,\mathrm{miss}}_{\mathrm{T}}, \ell) > 0.8$. In the e$\nu$jj channel, the angular separation ΔR between the electron and either of the jets is required to be larger than 0.7 in order to reduce the contamination from QCD multijet background in that channel. Events are required to have $M_{\mathrm{T}} > 50\,\mathrm{GeV}$, where M_{T}, the transverse mass of the charged lepton and undetected particles, is defined as $M_{\mathrm{T}} = \sqrt{2p^{\ell}_{\mathrm{T}}E^{\mathrm{miss}}_{\mathrm{T}}\,(1-\cos\Delta\phi)}$, where p^{ℓ}_{T} is the lepton p_{T} and $\Delta\phi$ is the difference in azimuthal angle between the charged lepton momentum direction and the $\vec{p}^{\,\mathrm{miss}}_{\mathrm{T}}$ vector. Lastly, events are selected to have $S_{\mathrm{T}} > 300\,\mathrm{GeV}$, where the scalar transverse energy S_{T} is defined in this case to be $S_{\mathrm{T}} = p_{\mathrm{T}}(\ell) + E^{\mathrm{miss}}_{\mathrm{T}} + p_{\mathrm{T}}(\mathrm{j}_1) + p_{\mathrm{T}}(\mathrm{j}_2)$.

After this initial selection, the following variables are used to optimize a final selection for each LQ mass hypothesis using the method described above: M_{T}; S_{T}; and $M_{\ell\mathrm{j}}$, defined as the invariant mass of the lepton-jet pair that minimizes the difference in the M_{T} of the lepton-jet and $E^{\mathrm{miss}}_{\mathrm{T}}$-jet pairs. The e$\nu$jj channel uses $E^{\mathrm{miss}}_{\mathrm{T}}$ as an additional optimization variable.

The optimized thresholds for the eνjj and the $\mu\nu$jj channels are summarized in Tables 3 and 4, respectively. Mass hypotheses beyond 950 (1000) GeV for the eνjj ($\mu\nu$jj) channel use the same set of final selections as those for the 950 (1000) GeV mass hypothesis.

Table 3: Optimized thresholds for different LQ mass hypotheses of the eνjj signal.

	LQ Mass [GeV]													
	300	350	400	450	500	550	600	650	700	750	800	850	900	$\geq$950
S_T [GeV]	495	570	645	720	800	880	960	1040	1120	1205	1290	1375	1460	1545
M_{ej} [GeV]	195	250	300	355	405	455	505	555	600	645	695	740	780	825
M_T [GeV]	125	150	175	200	220	240	255	270	280	290	295	300	300	300
E_T^{miss} [GeV]	90	95	100	110	115	125	135	145	155	170	180	195	210	220

Table 4: Optimized thresholds for different LQ mass hypotheses of the $\mu\nu$jj signal.

	LQ Mass [GeV]														
	300	350	400	450	500	550	600	650	700	750	800	850	900	950	$\geq$1000
S_T [GeV]	455	540	625	715	800	890	980	1070	1160	1250	1345	1435	1530	1625	1720
$M_{\mu j}$ [GeV]	125	150	175	200	225	250	280	305	330	355	380	410	435	465	490
M_T [GeV]	155	180	205	225	245	260	275	290	300	310	315	320	320	325	320

5 Background estimation

The main SM processes that can mimic the LQ signal in the $\ell\ell$jj channels are: processes that lead to the production of genuine dilepton events such as Z/γ^*+jets, $t\bar{t}$, and VV+jets; and processes which produce either 0 or 1 genuine leptons and at least one hadronic jet which leads to a mis-identified lepton such as multijet events, single t production, and W+jets. The contributions from single top quarks, VV+jets, and W+jets are estimated from simulation and are small once the full event selection is applied. The contribution from the principal background, Z/γ^*+jets, is estimated with using simulated events normalized to the data in a control region, where the non-Z/γ^*+jets backgrounds have been removed from the data control region using the identical selection in simulation. The Z/γ^*+jets simulation is rescaled to agree with this modified data sample at the $\ell\ell$jj initial selection level within a Z boson enriched region of 70 (80) $< M_{\ell\ell} <$ 110 (100) GeV for the electron (muon) channel. The resulting correction factor is $R_Z = 0.97 \pm 0.01$ (stat) for eejj, and $R_Z = 0.92 \pm 0.01$ (stat) for $\mu\mu$jj. The contribution from $t\bar{t}$ events with two leptons of the same flavor is estimated from a data sample containing one electron and one muon. This data sample is dominated by $t\bar{t}$ processes, which are expected to yield eμjj events with the same probability as (eejj + $\mu\mu$jj) events. The data sample is therefore reweighted to account for: the different branching fraction of the eμjj final state, which is twice that of the eejj or $\mu\mu$jj final states; the differences in electron and muon identification and isolation efficiencies; and the differences in trigger efficiencies. This sample can then be used to estimate the contribution from the $t\bar{t}$ process in the $\ell\ell$jj channels for both the initial and final selections in all kinematic distributions.

The multijet background in the eejj channel is determined from a data control region containing exactly two electron candidates that pass loosened identification criteria on the cluster shape and no isolation requirements, and at least two jets. Each electron candidate in this sample is weighted by the probability that an electron candidate passing such loosened requirements additionally passes all final electron requirements. This probability is measured as a function of p_T in three η regions ($|\eta| < 1.442$, $1.56 < |\eta| < 2.00$, and $2.00 < |\eta| < 2.50$), using a data sample dominated by multijet events, collected with a single-photon trigger and containing one and only one electron candidate and two or more jets. The contribution from multijet processes in the $\mu\mu$jj channel is determined using a multijet-enriched data sample of same-sign dimuon events with no muon isolation criteria imposed. The same-sign nonisolated data sample is reweighted according to a same-sign/opposite-sign ratio and an isolation acceptance factor calculated using simulation. After reweighting, the same-sign nonisolated data sample is used to predict the multijet contribution to the final $\mu\mu$jj selection, which is shown to be negligible.

All final state distributions in the eejj and $\mu\mu$jj channels of the background prediction and of

data, at the initial selection level, have been studied and show agreement within uncertainties. The specific distributions of S_T and $M_{\ell j}^{min}$ are shown in Fig. 3. Systematic uncertainties, discussed in the next section, are not included in these plots.

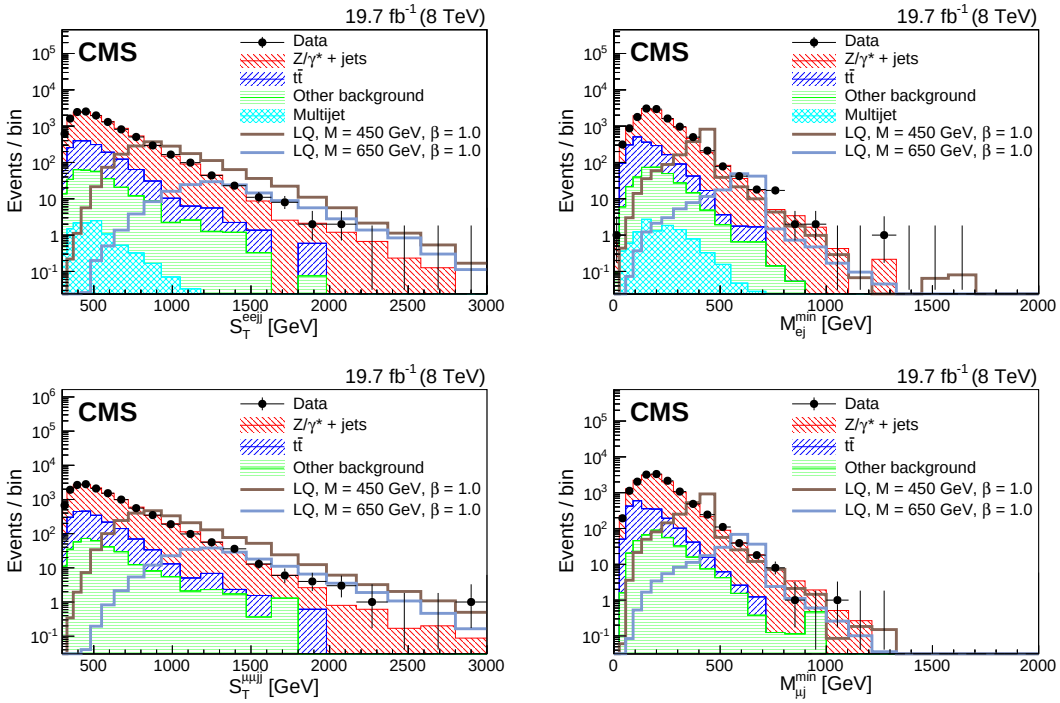

Figure 3: Distributions of S_T (left) and $M_{\ell j}^{min}$ (right) at the initial selection level in the eejj (top) and $\mu\mu$jj (bottom) channels. "Other background" includes: diboson, W+jets, γ+jets, and single top quark contributions. The horizontal lines on the data points show the variable bin width.

The primary backgrounds that can mimic the LQ signal in the $\ell\nu$jj channels fall into three categories: events with genuine W bosons such as those from W+jets, $t\bar{t}$, single top quark production, and WW and WZ processes; events with misidentified leptons and misreconstructed E_T^{miss} in the final state caused mostly by the misidentification of jets as leptons in multijet processes; and events with Z bosons such as those from Z/γ^*+jets and ZZ processes, where only one lepton passes the identification and selection requirements.

The contributions from the leading backgrounds (W+jets and $t\bar{t}$) are determined using simulated events normalized to the data in control regions. The signal-depleted region $70 < M_T < 110$ GeV is used to determine both the W+jets and the $t\bar{t}$ normalization factors using two mutually exclusive selections. Selecting events with fewer than four jets produces a sample enhanced with W+jets, and selecting events with at least four jets produces a sample enhanced with $t\bar{t}$ events. The results of these two selections are used to derive normalization factors from the following set of equations:

$$\begin{aligned} N_1 &= R_{t\bar{t}} N_{1,t\bar{t}} + R_W N_{1,W} + N_{1,O} \\ N_2 &= R_{t\bar{t}} N_{2,t\bar{t}} + R_W N_{2,W} + N_{2,O} \end{aligned} \quad (1)$$

where N_i, $N_{i,t\bar{t}}$, $N_{i,W}$, and $N_{i,O}$ are the number of events in data, W+jets, $t\bar{t}$, and other backgrounds passing selection i. The solution of the system yields the following normalization factors for the $\mu\nu$jj channel: $R_{t\bar{t}} = 0.99 \pm 0.02$ (stat) and $R_W = 0.95 \pm 0.01$ (stat). Similar factors are obtained for the $e\nu$jj channel: $R_{t\bar{t}} = 0.97 \pm 0.02$ (stat) $\pm$ 0.01 (syst) and $R_W =$

0.85 ± 0.01 (stat) $\pm$ 0.01 (syst), where the systematic uncertainties are associated with the estimate of the multijet background in this particular channel. The value of R_W in the eνjj channel is affected by the lower efficiency of the trigger used in selecting W+jets events.

The multijet background in the eνjj channel is determined from data, using the previously described probability that an electron candidate satisfying loosened requirements also passes the final electron requirements. The probability is used to weight a sample of events containing: exactly one electron candidate passing the loosened identification criteria, at least two jets, and large E_T^{miss}. The contribution from multijet processes is determined in the $\mu\nu$jj channel using a sample of muon-enriched multijet simulated events with no muon isolation condition imposed. In the multijet-enriched region with $E_T^{miss} < 10\,GeV$, the muon-enriched multijet simulated events are reweighted to agree with data, and a muon isolation acceptance rate is calculated using the data as the number of events passing the isolation condition divided by the total number of events. After reweighting and an adjustment by the muon isolation acceptance factor, the nonisolated muon-enriched multijet simulated events are used to estimate the multijet contribution passing the final selection, which is determined in the $\mu\nu$jj channel to be negligible.

The contribution from the remaining backgrounds (diboson, single top quark, and Z/γ^*+jets) is small and is determined entirely from simulation.

As with the eejj and $\mu\mu$jj channels, all final state distributions in the eνjj and $\mu\nu$jj channels of the background prediction and of data, at the initial selection level, have been studied and also show agreement within uncertainties. The specific distributions of S_T and $M_{\ell j}^{min}$ for these channels are shown in Fig. 4. Systematic uncertainties, discussed in the next section, are not included in these plots.

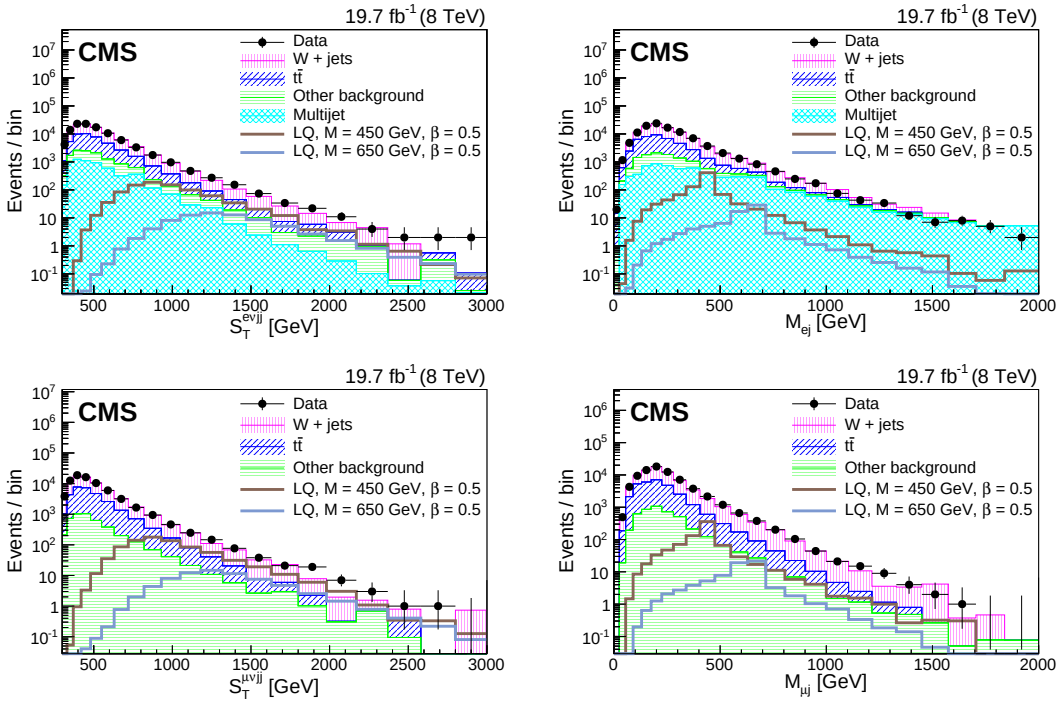

Figure 4: Distributions of S_T (left), and $M_{\ell j}$ (right) at the initial selection level in the eνjj (top) and $\mu\nu$jj (bottom) channels. "Other background" includes: diboson, Z/γ^*+jets, and single top quark contributions. The horizontal lines on the data points show the variable bin width.

6 Systematic uncertainties

The sources of systematic uncertainty considered in this analysis are described below. To determine the final uncertainty in signal and background predictions, each quantity is individually varied within its uncertainty, and the entire analysis is repeated to find the change in the predicted number of background and signal events.

The dominant sources of systematic uncertainty are the jet energy scale and resolution uncertainties, which are estimated by assigning a p_T- and η-dependent uncertainty in jet energy corrections, as described in Ref. [69], and by varying the jet p_T by the uncertainty. The uncertainties in jet energy resolution are assessed by modifying the p_T difference between the reconstructed and particle-level jets by an η-dependent value [69] ranging between 5% and 30% for most jets. Charged-lepton momentum scale and resolution uncertainties also introduce uncertainties in the overall event acceptance. A p_T-dependent muon momentum uncertainty of $5\% \times (p_T)$, where p_T is expressed in TeV, and a p_T-dependent muon momentum resolution uncertainty ranging between 1 and 4% are used [63]. For electrons in the ECAL barrel and endcap region, an energy scale uncertainty of 2% [70] and an electron energy resolution uncertainty of 10% [40] are used. The effects of these uncertainties are assessed by modifying the electron momentum scale and resolution in the simulation according to these uncertainties. A 2% per muon uncertainty in the muon reconstruction, identification, and isolation requirements, and a 1% per muon uncertainty in the muon HLT efficiency are assigned in the $\mu\mu$jj and $\mu\nu$jj channels. An additional uncertainty is assigned for the $\mu\mu$jj and $\mu\nu$jj channels because of the effect on the muon momentum determination of the uncertainty on the alignment of the muon system. In simulation, a ϕ modulation can be seen in the difference between the inverse of the muon momentum as determined by the tracker with that determined by the tracker plus the muon system. Corrections were derived, but produced minimal differences, so instead a small uncertainty is added to account for possible alignment effects. In the $\ell\nu$jj analyses, the uncertainty in the charged lepton and jet energy and momentum scales and resolutions are propagated to the measurement of E_T^{miss}.

Other important sources of systematic uncertainty are related to the modeling of the backgrounds in the simulation. The uncertainties in the Z/γ^*+jets, W+jets, and $t\bar{t}$ background shapes are determined using simulated MADGRAPH samples for which the renormalization and factorization scales and matrix element to parton shower matching thresholds have been varied up and down by a factor of two. The uncertainty of the scale factors for the normalization of the Z/γ^*+jets background is determined to be 1% in both $\ell\ell$jj channels. A similar uncertainty for the normalization of the W+jets background is determined to be $2\%(1\%)$ in the eνjj ($\mu\nu$jj) channel. The scale factor for the normalization of the $t\bar{t}$ background is determined to have an uncertainty of 2% in the eνjj and $\mu\nu$jj channels. The scale factor for the normalization of the eμjj sample used for the $t\bar{t}$ background estimate in the eejj channel is determined to have an 8% uncertainty.

The estimate of the multijet background from data in the eejj (eνjj) channel has an uncertainty of 60% (30%). This uncertainty is assessed by probing the precision of the method used to measure this type of background on an independent data control sample.

An uncertainty in the modeling of pileup is determined by re-weighting the MC events to match with a number of pileup events 6% larger or smaller than what is observed in data, and an uncertainty of 2.6% is assigned to the value of the integrated luminosity [41].

Lastly, the uncertainty in the signal acceptance, background acceptance, and cross section due to the PDF choice is estimated for signal (background) to be: 2% (3%) in the eejj channel; 3%

(3-25%) in the eνjj channel; 2% (2-12%) in the $\mu\mu$jj channel; and 2% (1-21%) in the $\mu\nu$jj channel, following the PDF4LHC procedure [71, 72].

The systematic uncertainties for both signal and background are summarized in Table 5 for all channels, corresponding to the final selection optimized for $M_{\mathrm{LQ}} = 650\,\mathrm{GeV}$, which is representative of other high mass LQ values.

Table 5: Systematic uncertainties (in %) for signal (S) and background (B) in all channels for the $M_{\mathrm{LQ}} = 650\,\mathrm{GeV}$ final selection.

Systematic	eejj		$\mu\mu$jj		eνjj		$\mu\nu$jj	
Uncertainties	S [%]	B [%]	S [%]	B [%]	S [%]	B [%]	S [%]	B [%]
Jet energy scale	0.30	0.52	0.42	0.14	1.6	2.2	0.02	1.9
Electron energy scale	0.97	6.4	—	—	2.8	3.3	—	—
Electron Reco/ID/Iso	4.0	<0.01	—	—	2.0	<0.01	—	—
Muon momentum scale	—	—	0.63	1.7	—	—	0.19	13
Muon Reco/ID/Iso	—	—	4	0.48	—	—	2.0	0.19
Jet resolution	0.01	0.23	0.23	0.86	0.09	0.46	0.78	2.2
Electron resolution	0.46	0.22	—	—	0.61	0.53	—	—
Muon resolution	—	—	0.14	0.39	—	—	0.15	7.1
Muon alignment	—	—	0.1	0.54	—	—	1.0	2.8
Trigger	<0.01	<0.01	<0.01	<0.01	<0.01	<0.01	1.0	0.10
$\mathrm{t\bar{t}}$ normalization	—	2.1	—	0.35	—	1.5	—	0.60
$\mathrm{t\bar{t}}$ shape	—	—	—	—	—	3.0	—	1.4
W+jets normalization	—	<0.01	—	0.01	—	0.12	—	0.63
W+jets shape	—	<0.01	—	0.23	—	0.87	—	13
Z/γ^*+jets normalization	—	0.75	—	0.59	—	<0.01	—	0.07
Z/γ^*+jets shape	—	12	—	12	—	<0.01	—	1.5
Multijet modeling	—	0.10	—	—	—	5	—	—
PDF	2.0	2.1	2.0	4.8	3.0	13	3.0	5.1
Pileup	0.04	0.38	0.16	0.22	0.14	1.2	0.06	1.3
Integrated luminosity	2.6	0.10	2.6	0.31	2.6	0.47	2.6	0.25
Total	5.3	14	5.2	13	5.5	15	4.7	21

7 Results

Data and background predictions are compared for every channel and each mass optimization point, after the optimized final selection criteria are applied to both signal and background. The first part of this section details such comparisons. There are no significant deviations from SM background predictions. Limits are set on the cross section times branching fraction for the hypothesis of scalar LQ pair production as a function of M_{LQ} and β. The expected and observed limits for scalar LQ pair production are detailed in the second part of this section. Additional interpretations of the results in the context of vector LQ pair production and of RPV SUSY production with $\ell\ell$jj and $\ell\nu$jj signatures are described in the last part of this section.

7.1 Data and background comparison

Agreement is found between data and background predictions in both the $\mu\mu$jj and $\mu\nu$jj channels, as shown in Fig. 5 for the $\mu\mu$jj channel, which displays S_{T} and $M_{\mu\mathrm{j}}^{\mathrm{min}}$ for signal LQ masses of 450 and 650 GeV, and in Fig. 6 for the $\mu\nu$jj channel, which displays S_{T} and $M_{\mu\mathrm{j}}$ for the same signal LQ mass points.

The numbers of events selected in data, and the various backgrounds at final selection as a function of M_{LQ} for the $\mu\mu$jj and $\mu\nu$jj channels are summarized in Tables 6 and 7, respectively.

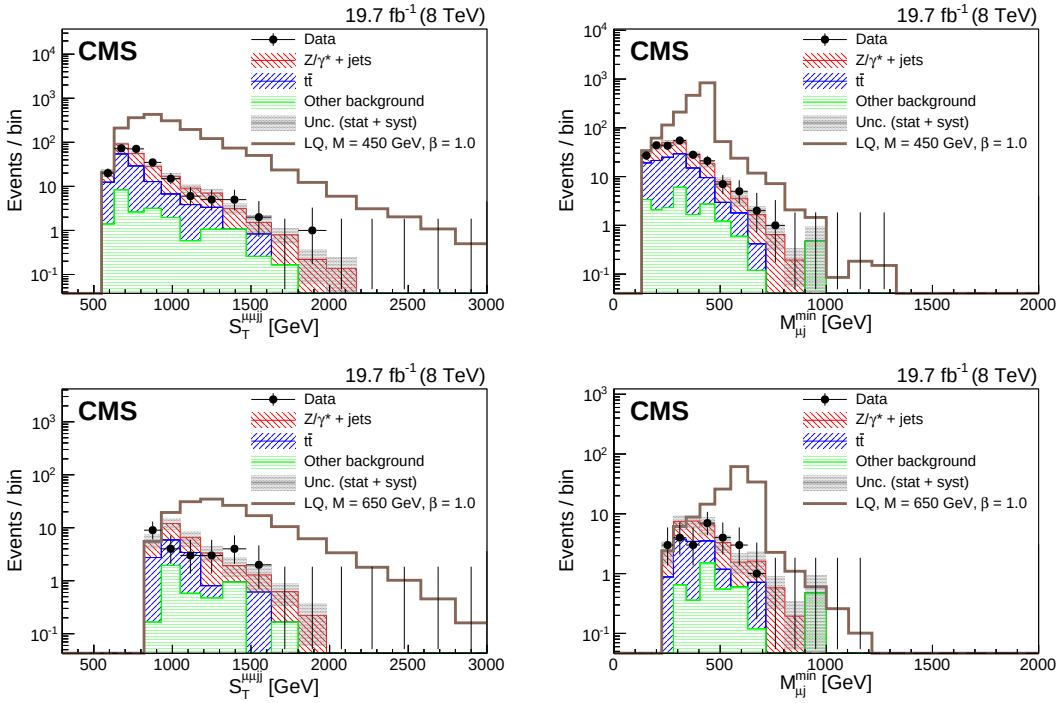

Figure 5: Distributions of S_{T} (left) and $M_{\mu\mathrm{j}}^{\mathrm{min}}$ (right) for the final selection for a LQ mass of 450 GeV (top) and 650 GeV (bottom) in the $\mu\mu$jj channel. The dark shaded region indicates the statistical and systematic uncertainty in the total background prediction. "Other background" includes diboson, W+jets, and single top quark contributions. The horizontal lines on the data points show the variable bin width.

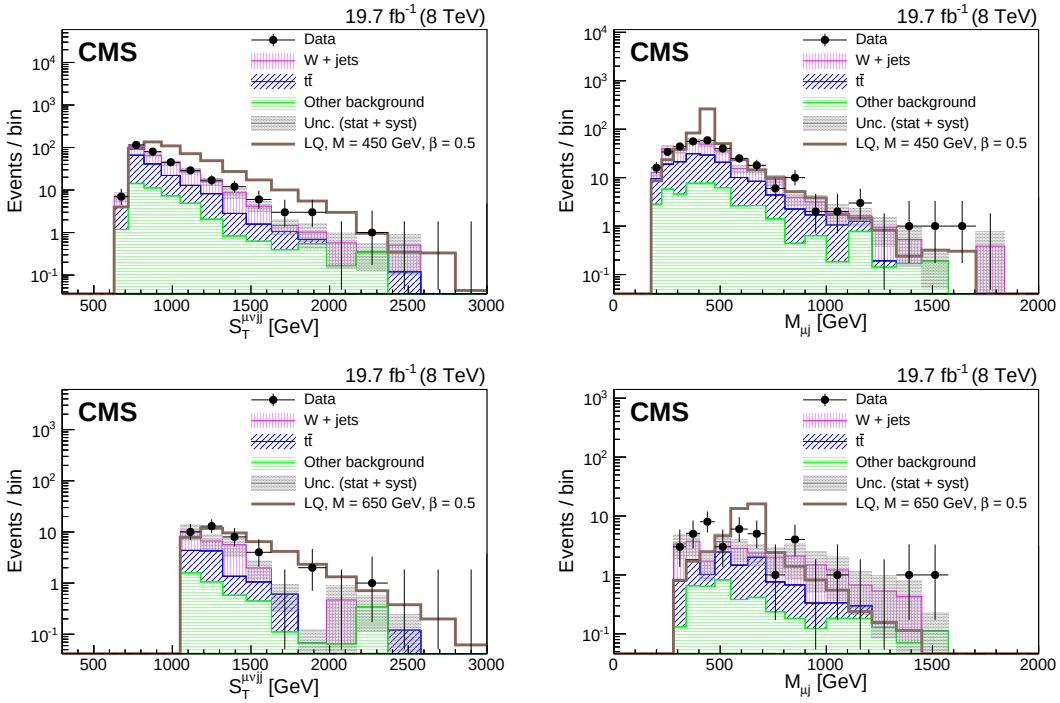

Figure 6: Distributions of S_{T} (left) and $M_{\mu\mathrm{j}}$ (right) for the final selection for a LQ mass of 450 GeV (top) and 650 GeV (bottom) in the $\mu\nu$jj channel. The dark shaded region indicates the statistical and systematic uncertainty in the total background prediction. "Other background" includes diboson, Z/γ^{*}+jets, and single top quark contributions. The horizontal lines on the data points show the variable bin width.

Since mass hypotheses at 1 TeV and beyond share the same final selections, they also share the same background yields.

Table 6: Event yields for the $\mu\mu$jj analysis for $\beta = 1.0$ for all values of M_{LQ}. Uncertainties are Poisson uncertainties in the simulated background, except for the second uncertainty for "All background", which gives the total systematic uncertainty as detailed in Section 6. Systematic uncertainties are dominated by jet energy scale and simulation shape uncertainties.

M_{LQ} [GeV]	Signal	Z/γ^*+jets	$t\bar{t}$	VV, W, single t	All background	Data
300	16240 ± 110	819.0 ± 9.2	666 ± 19	88 ± 5.4	1573 ± 22 ± 56	1659
350	7570 ± 48	351.7 ± 6.0	405 ± 15	58.3 ± 4.5	815 ± 17 ± 21	797
400	3658 ± 22	200.4 ± 4.5	202 ± 11	31.5 ± 3.3	434 ± 12 ± 17	439
450	1816 ± 11	110.2 ± 3.3	103.7 ± 27.5	20.6 ± 2.7	234.6 ± 8.6 ± 11.2	233
500	938.1 ± 5.5	69.9 ± 2.6	61.0 ± 5.7	13.2 ± 2.2	144.2 ± 6.7 ± 8.5	135
550	498.8 ± 2.9	39.6 ± 1.9	29.4 ± 3.9	8.0 ± 1.8	77 ± 4.7 ± 5.2	84
600	274.7 ± 1.6	25.8 ± 1.5	14.8 ± 2.8	6.5 ± 1.6	47.1 ± 3.6 ± 4.5	47
650	157.1 ± 0.9	17.1 ± 1.2	10.3 ± 2.3	$4.3^{+1.4}_{-1.3}$	$31.7^{+2.9}_{-2.9}$ ± 4.2	25
700	89.49 ± 0.52	10.71 ± 0.98	7.0 ± 2.0	$2.9^{+1.2}_{-1.0}$	$20.6^{+2.5}_{-2.4}$ ± 4.3	15
750	52.39 ± 0.30	6.95 ± 0.79	2.20 ± 0.98	$1.1^{+0.8}_{-0.56}$	$10.3^{+1.5}_{-1.4}$ ± 2.7	11
800	31.3 ± 0.18	3.90 ± 0.59	1.08 ± 0.62	$0.77^{+0.73}_{-0.46}$	$5.8^{+1.1}_{-1.0}$ ± 1.55	9
850	18.99 ± 0.11	1.96 ± 0.39	$0.0^{+0.65}_{-0.0}$	$0.75^{+0.73}_{-0.46}$	$2.71^{+0.97}_{-0.65}$ ± 1.07	5
900	11.290 ± 0.067	1.10 ± 0.29	$0.0^{+0.65}_{-0.0}$	$0.30^{+0.60}_{-0.20}$	$1.38^{+0.82}_{-0.40}$ ± 0.44	3
950	6.907 ± 0.041	0.76 ± 0.25	$0.0^{+0.65}_{-0.0}$	$0.12^{+0.78}_{-0.12}$	$0.87^{+0.85}_{-0.32}$ ± 0.49	1
1000	4.175 ± 0.026	0.41 ± 0.18	$0.0^{+0.65}_{-0.0}$	$0.0^{+0.77}_{-0.0}$	$0.41^{+0.91}_{-0.18}$ ± 0.27	0
1050	2.778 ± 0.017	0.41 ± 0.18	$0.0^{+0.65}_{-0.0}$	$0.0^{+0.77}_{-0.0}$	$0.41^{+0.91}_{-0.18}$ ± 0.27	0
1100	1.860 ± 0.011	0.41 ± 0.18	$0.0^{+0.65}_{-0.0}$	$0.0^{+0.77}_{-0.0}$	$0.41^{+0.91}_{-0.18}$ ± 0.27	0
1150	1.2471 ± 0.0072	0.41 ± 0.18	$0.0^{+0.65}_{-0.0}$	$0.0^{+0.77}_{-0.0}$	$0.41^{+0.91}_{-0.18}$ ± 0.27	0
1200	0.8202 ± 0.0047	0.41 ± 0.18	$0.0^{+0.65}_{-0.0}$	$0.0^{+0.77}_{-0.0}$	$0.41^{+0.91}_{-0.18}$ ± 0.27	0

In both the eejj and eνjj channels, a broad data excess is observed for the selections optimized for a LQ mass greater than about 400 GeV, as shown in Figs. 7 and 8 for two chosen selections, and in Tables 8 and 9. This excess is most significant in the selection optimized for a LQ mass of 650 GeV, where for the eejj (eνjj) channel 20.5 ± 2.1 (stat) ± 2.8 (syst) (7.5 ± 1.2 (stat) $\pm$ 1.1 (syst)) events are expected and 36 (18) events are observed, with a significance of 2.3 (2.6) standard deviations.

An investigation of the kinematic distributions in both channels shows that the excesses are background-like. In particular, unlike a LQ hypothesis, the excesses do not peak sharply in the $M_{\mathrm{ej}}^{\mathrm{min}}$ and the M_{ej} distributions, as shown in Fig. 9. For comparison, the distributions that would result from a LQ mass hypothesis of 650 GeV and $\beta = 0.075$ are also shown (this is the value of β that, for a LQ mass of 650 GeV, would produce 10 events in the eνjj selection optimized for such a LQ mass, which is about the size of the excess). The intrinsic width of scalar LQs is $\frac{\lambda_{\ell q}^2}{16\pi} \times M_{\mathrm{LQ}}$. The LQ signal events were generated with $\lambda_{\ell q} = 0.3$. This corresponds to an intrinsic width of about 1.2 GeV for a LQ with mass close to 650 GeV, which is negligible compared to the experimental resolution. Significantly higher values of $\lambda_{\ell q}$ (and consequently broader LQs) are strongly limited in this mass range by results from the HERA experiments [27, 28].

Further investigations of the characteristics of the data that survives the selections optimized for a LQ mass of 650 GeV show that there are two events containing same-sign electrons out of the 36 events, and we expect the SM background to contribute about two events with same-sign electrons out of the about 20 predicted events, because of charge misidentification. We

Table 7: Event yields for the $\mu\nu$jj analysis for $\beta = 0.5$ for all values of M_{LQ}. Uncertainties are Poisson uncertainties in the simulated background, except for the second uncertainty for "All background", which gives the total systematic uncertainty as detailed in Section 6. Systematic uncertainties are dominated by the jet energy scale and simulation shape uncertainties.

M_{LQ} [GeV]	Signal	W+jets	$t\bar{t}$	VV, Z, single t	All background	Data
300	5089 ± 58	1102 ± 22	1853 ± 15	331.3 ± 8.3	3286 ± 28 ± 185	3549
350	2352 ± 25	472 ± 14	640.0 ± 8.5	159.8 ± 5.7	1272 ± 18 ± 70	1451
400	1064 ± 11	213.9 ± 9.6	259.5 ± 5.4	84.6 ± 4.3	558 ± 12 ± 38	668
450	526.7 ± 5.5	115.7 ± 7.1	116.3 ± 3.6	44.8 ± 2.9	276.7 ± 8.5 ± 22	313
500	263.6 ± 2.8	66.4 ± 5.3	56.1 ± 2.5	25.1 ± 2.1	147.6 ± 6.2 ± 12.6	173
550	142.7 ± 1.5	43.8 ± 4.4	26.1 ± 1.7	14.3 ± 1.6	84.3 ± 5.0 ± 9.4	93
600	78.1 ± 0.8	20.3 ± 2.7	13.7 ± 1.2	8.0 ± 1.1	42 ± 3.2 ± 5.8	57
650	44.62 ± 0.46	14.0 ± 2.3	7.97 ± 0.95	4.34 ± 0.72	26.3 ± 2.6 ± 5.2	36
700	25.27 ± 0.26	9.1 ± 1.8	5.20 ± 0.76	$2.73^{+0.64}_{-0.46}$	17 ± 2.0 ± 4.7	25
750	15.04 ± 0.15	7.0 ± 1.6	2.82 ± 0.56	$1.93^{+0.60}_{-0.40}$	11.7 ± 1.8 ± 5.1	15
800	9.080 ± 0.093	4.5 ± 1.4	1.47 ± 0.41	$1.61^{+0.58}_{-0.37}$	7.6 ± 1.5 ± 3.5	11
850	5.493 ± 0.056	1.08 ± 0.54	1.04 ± 0.35	$1.16^{+0.55}_{-0.32}$	$3.28^{+0.81}_{-0.74}$ ± 1.04	7
900	3.370 ± 0.035	0.62 ± 0.44	0.92 ± 0.32	$0.9^{+0.53}_{-0.29}$	$2.44^{+0.72}_{-0.64}$ ± 0.89	3
950	2.111 ± 0.022	0.4 ± 0.4	0.44 ± 0.22	$0.51^{+0.49}_{-0.21}$	$1.35^{+0.62}_{-0.52}$ ± 0.6	3
1000	1.322 ± 0.014	0.4 ± 0.4	0.26 ± 0.18	$0.51^{+0.49}_{-0.21}$	$1.17^{+0.61}_{-0.51}$ ± 0.56	3
1050	0.9338 ± 0.0092	0.4 ± 0.4	0.26 ± 0.18	$0.51^{+0.49}_{-0.21}$	$1.17^{+0.61}_{-0.51}$ ± 0.56	3
1100	0.6507 ± 0.0062	0.4 ± 0.4	0.26 ± 0.18	$0.51^{+0.49}_{-0.21}$	$1.17^{+0.61}_{-0.51}$ ± 0.56	3
1150	0.4457 ± 0.0041	0.4 ± 0.4	0.26 ± 0.18	$0.51^{+0.49}_{-0.21}$	$1.17^{+0.61}_{-0.51}$ ± 0.56	3
1200	0.3097 ± 0.0028	0.4 ± 0.4	0.26 ± 0.18	$0.51^{+0.49}_{-0.21}$	$1.17^{+0.61}_{-0.51}$ ± 0.56	3

have also verified that the excess is not enhanced if we require that the jets are identified as b-quark jets using the combined secondary vertex b-tagging algorithm [73].

A recently published search for heavy neutrinos and W bosons with right-handed couplings [74] also observed an excess in the number of selected eejj events compared to the expectation from SM backgrounds. However, the excess in Ref. [74] is mostly localized in the region $1.8 < M_{eejj} < 2.2$ TeV, where M_{eejj} is the invariant mass of the 2 leading electrons and 2 leading jets, while the excess observed in this analysis with the selection optimized for LQ mass of 650 GeV is broadly distributed between M_{eejj} values of 1 and 2 TeV. Furthermore, only 30% of the events populating the excess region in Ref. [74] survive the $M_{LQ} = 650$ GeV selection.

In summary, the kinematic properties of the data in the excess regions for the eejj and the eνjj channels are not found to be consistent with a LQ signal, and the size of the data excess is significantly less than that expected for a LQ with a mass of 650 GeV and $\beta \geq 0.5$. In the following section, limits are set on LQ production for both first and second generation.

7.2 Exclusion limits on scalar LQ pair-production

Upper limits are set on the scalar LQ production cross sections σ using the asymptotic CL_S modified-frequentist approach [75, 76]. A log-normal probability density function is used to integrate over the systematic uncertainties described in Section 6. Uncertainties of statistical nature are described with gamma distributions with widths determined by the number of events in signal and background simulated samples or observed in data control regions.

The 95% confidence level (CL) upper limits on $\sigma \times \beta^2$ or $\sigma \times 2\beta(1-\beta)$ as a function of LQ mass are shown together with the NLO predictions for the scalar LQ pair production cross section in Fig. 10 for the eejj and eνjj channels, and in Fig. 11 for the $\mu\mu$jj and $\mu\nu$jj channels.

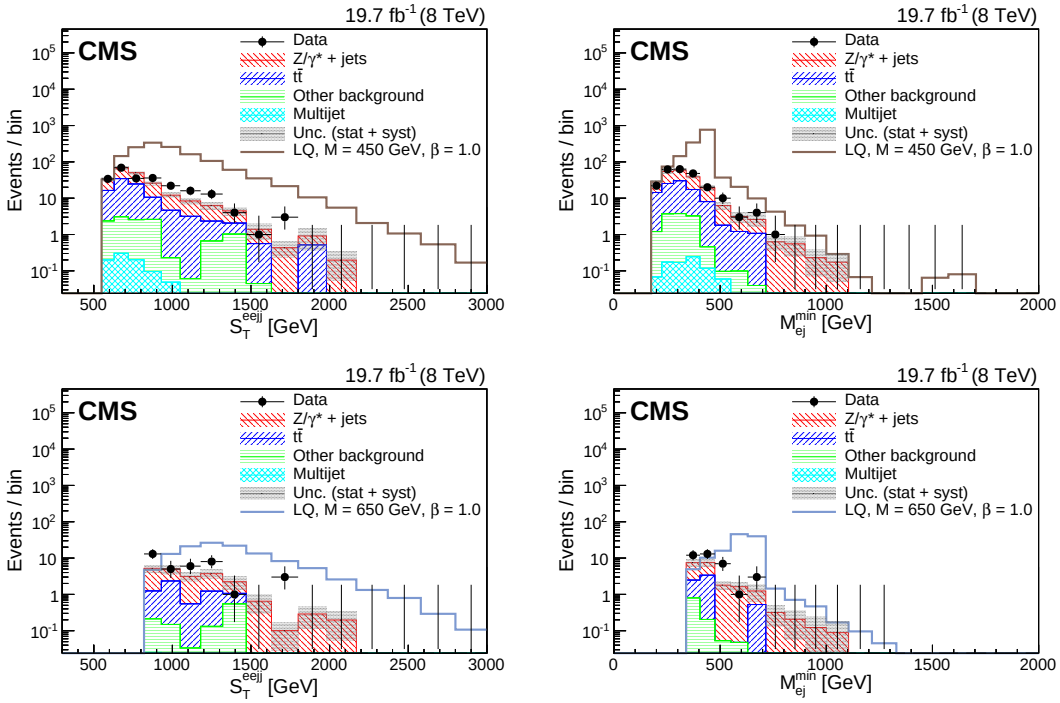

Figure 7: The S_{T} (left) and $M_{\mathrm{ej}}^{\mathrm{min}}$ (right) distributions for events passing the eejj selection optimized for $M_{\mathrm{LQ}} = 450\,\mathrm{GeV}$ (top) and $M_{\mathrm{LQ}} = 650\,\mathrm{GeV}$ (bottom). The dark shaded region indicates the statistical and systematic uncertainty in the background total prediction. "Other background" includes diboson, W+jets, and single top quark contributions. The horizontal lines on the data points show the variable bin width.

Table 8: Event yields for the eejj analysis for $\beta = 1.0$ for all values of M_{LQ}. Only statistical uncertainties are reported, except in the "All background" column, where systematic uncertainties are also reported.

M_{LQ} [GeV]	Signal	Z/γ^*+jets	$\mathrm{t\bar{t}}$	Multijet	VV, W, single t	All background	Data
300	13560 ± 80	462.2 ± 7.4	724 ± 20	5.280 ± 0.052	62.1 ± 4.6	1254 ± 22 ± 76	1244
350	6474 ± 33	332.1 ± 6.2	352 ± 14	3.220 ± 0.036	37.7 ± 3.6	725 ± 16 ± 48	736
400	3089 ± 15	203.2 ± 4.8	153.7 ± 9.1	1.700 ± 0.023	23.8 ± 2.9	382 ± 11 ± 27	389
450	1508 ± 7.2	112.9 ± 3.5	86.9 ± 6.9	0.890 ± 0.016	11.8 ± 2.0	212 ± 8.0 ± 18	233
500	767.4 ± 3.6	66.5 ± 2.7	47.2 ± 5.1	0.490 ± 0.011	7.4 ± 1.6	122 ± 6.0 ± 9.3	148
550	410.5 ± 1.9	37.4 ± 2.1	25.8 ± 3.7	0.2800 ± 0.0084	3.7 ± 1.1	67.2 ± 4.4 ± 5.2	81
600	225.7 ± 1.0	22.2 ± 1.6	14.2 ± 2.8	0.1500 ± 0.0065	3.12 ± 1.00	39.7 ± 3.4 ± 3.3	57
650	125.90 ± 0.58	14.0 ± 1.2	5.4 ± 1.7	0.0760 ± 0.0040	1.05 ± 0.47	20.5 ± 2.1 ± 2.8	36
700	72.88 ± 0.33	8.16 ± 0.93	4.3 ± 1.5	0.0450 ± 0.0029	0.21 ± 0.12	12.7 ± 1.8 ± 2.3	17
750	43.10 ± 0.20	4.88 ± 0.69	1.55 ± 0.90	0.0260 ± 0.0023	0.078 ± 0.038	6.5 ± 1.1 ± 1.2	12
800	26.17 ± 0.12	2.93 ± 0.52	1.04 ± 0.73	0.0190 ± 0.0022	0.078 ± 0.038	4.06 ± 0.90 ± 0.93	7
850	15.980 ± 0.072	2.34 ± 0.48	0.52 ± 0.52	0.0110 ± 0.0015	0.042 ± 0.028	2.91 ± 0.71 ± 0.74	5
900	9.813 ± 0.044	1.23 ± 0.36	0.52 ± 0.52	0.0069 ± 0.0012	0.022 ± 0.020	1.77 ± 0.63 ± 0.39	3
950	6.086 ± 0.028	0.89 ± 0.29	$0.00\,^{+1.14}_{-0}$	0.00450 ± 0.00085	0.022 ± 0.020	$0.91\,^{+1.18}_{-0.30}$ ± 0.28	1
1000	3.860 ± 0.018	0.56 ± 0.22	$0.00\,^{+1.14}_{-0}$	0.00370 ± 0.00082	0.0025 ± 0.0025	$0.57\,^{+1.16}_{-0.22}$ ± 0.18	1
1050	2.576 ± 0.011	0.56 ± 0.22	$0.00\,^{+1.14}_{-0}$	0.00370 ± 0.00082	0.0025 ± 0.0025	$0.57\,^{+1.16}_{-0.22}$ ± 0.18	1
1100	1.6940 ± 0.0072	0.56 ± 0.22	$0.00\,^{+1.14}_{-0}$	0.00370 ± 0.00082	0.0025 ± 0.0025	$0.57\,^{+1.16}_{-0.22}$ ± 0.18	1
1150	1.1270 ± 0.0047	0.56 ± 0.22	$0.00\,^{+1.14}_{-0}$	0.00370 ± 0.00082	0.0025 ± 0.0025	$0.57\,^{+1.16}_{-0.22}$ ± 0.18	1
1200	0.7500 ± 0.0030	0.56 ± 0.22	$0.00\,^{+1.14}_{-0}$	0.00370 ± 0.00082	0.0025 ± 0.0025	$0.57\,^{+1.16}_{-0.22}$ ± 0.18	1

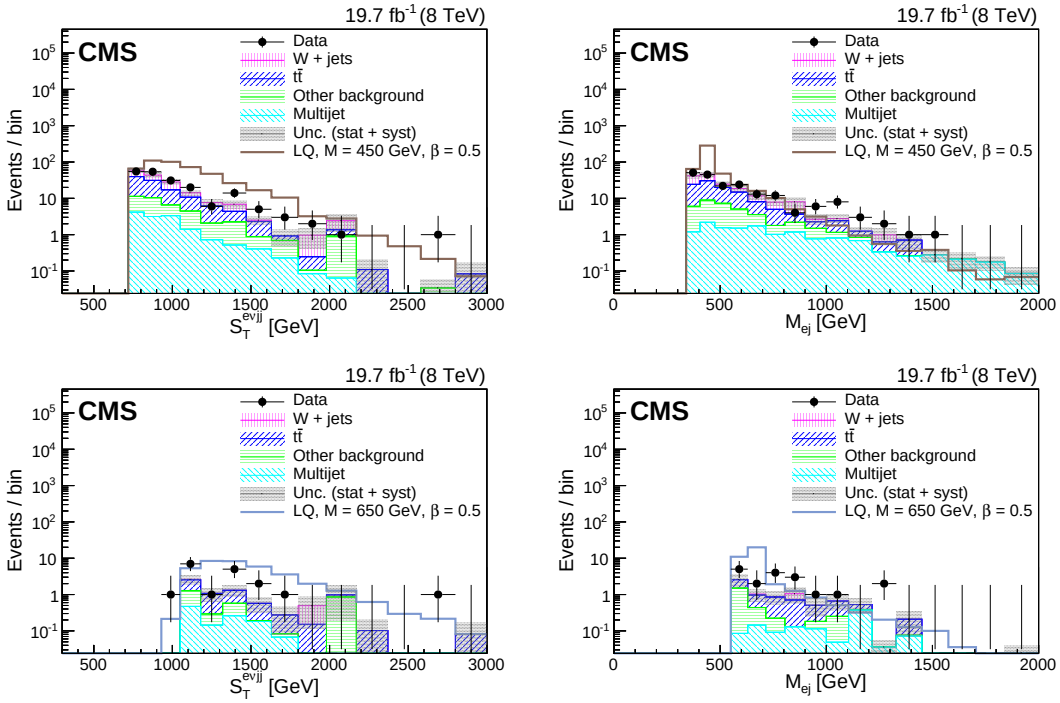

Figure 8: The S_{T} (left) and M_{ej} (right) distributions for events passing the full eνjj selection optimized for $M_{\mathrm{LQ}} = 450\,\mathrm{GeV}$ (top) and $M_{\mathrm{LQ}} = 650\,\mathrm{GeV}$ (bottom). The dark shaded region indicates the statistical and systematic uncertainty in the total background prediction. "Other background" includes diboson, Z/γ^{*}+jets, and single top quark contributions. The horizontal lines on the data points show the variable bin width.

Table 9: Event yields for the eνjj analysis for $\beta = 0.5$ for all values of M_{LQ}. Only statistical uncertainties are reported, except in the "All background" column, where systematic uncertainties are also reported.

M_{LQ} [GeV]	Signal	W+jets	$\mathrm{t\bar{t}}$	Multijet	VV, Z, single t	All background	Data
300	4642 ± 50	822 ± 22	1191 ± 12	117.9 ± 1.5	210.5 ± 7.7	2342 ± 27 ± 343	2455
350	2112 ± 21	276 ± 15	441.4 ± 7.2	59.11 ± 0.97	102.1 ± 5.4	879 ± 17 ± 127	908
400	945.8 ± 9.3	110.4 ± 7.8	184.2 ± 4.7	32.88 ± 0.69	51.5 ± 3.8	379.0 ± 9.9 ± 53.2	413
450	457.5 ± 4.5	53.1 ± 5.8	74.7 ± 3.0	14.13 ± 0.42	25.7 ± 2.7	167.6 ± 7.1 ± 22.2	192
500	226.7 ± 2.2	20.5 ± 3.3	34.4 ± 2.0	7.76 ± 0.30	15.3 ± 2.1	78.0 ± 4.4 ± 10.1	83
550	118.2 ± 1.2	8.6 ± 1.8	14.9 ± 1.4	3.89 ± 0.21	7.8 ± 1.6	35.4 ± 2.8 ± 4.5	44
600	64.65 ± 0.64	2.3 ± 1.0	7.08 ± 0.93	2.29 ± 0.17	4.6 ± 1.2	16.3 ± 1.8 ± 2.1	28
650	36.25 ± 0.36	0.41 ± 0.29	3.82 ± 0.70	1.18 ± 0.12	2.13 ± 0.92	7.5 ± 1.2 ± 1.1	18
700	21.18 ± 0.21	0.41 ± 0.29	2.61 ± 0.60	0.85 ± 0.10	0.58 ± 0.24	4.45 ± 0.71 ± 0.76	6
750	12.56 ± 0.12	$0.00\,^{+0.94}_{-0}$	1.75 ± 0.47	0.510 ± 0.091	0.27 ± 0.15	$2.54\,^{+1.07}_{-0.50}$ ± 0.50	4
800	7.412 ± 0.073	$0.00\,^{+0.94}_{-0}$	1.10 ± 0.37	0.317 ± 0.067	0.27 ± 0.15	$1.70\,^{+1.02}_{-0.41}$ ± 0.31	3
850	4.591 ± 0.045	$0.00\,^{+0.94}_{-0}$	0.90 ± 0.34	0.117 ± 0.029	0.140 ± 0.087	$1.15\,^{+1.00}_{-0.35}$ ± 0.24	2
900	2.853 ± 0.028	$0.00\,^{+0.94}_{-0}$	0.37 ± 0.21	0.076 ± 0.024	0.084 ± 0.069	$0.53\,^{+0.97}_{-0.22}$ ± 0.10	1
950	1.791 ± 0.017	$0.00\,^{+0.94}_{-0}$	0.37 ± 0.21	0.069 ± 0.023	0.084 ± 0.069	$0.52\,^{+0.97}_{-0.22}$ ± 0.10	1
1000	1.272 ± 0.011	$0.00\,^{+0.94}_{-0}$	0.37 ± 0.21	0.069 ± 0.023	0.084 ± 0.069	$0.52\,^{+0.97}_{-0.22}$ ± 0.10	1
1050	0.8788 ± 0.0074	$0.00\,^{+0.94}_{-0}$	0.37 ± 0.21	0.069 ± 0.023	0.084 ± 0.069	$0.52\,^{+0.97}_{-0.22}$ ± 0.10	1
1100	0.6063 ± 0.0049	$0.00\,^{+0.94}_{-0}$	0.37 ± 0.21	0.069 ± 0.023	0.084 ± 0.069	$0.52\,^{+0.97}_{-0.22}$ ± 0.10	1
1150	0.4196 ± 0.0032	$0.00\,^{+0.94}_{-0}$	0.37 ± 0.21	0.069 ± 0.023	0.084 ± 0.069	$0.52\,^{+0.97}_{-0.22}$ ± 0.10	1
1200	0.2894 ± 0.0021	$0.00\,^{+0.94}_{-0}$	0.37 ± 0.21	0.069 ± 0.023	0.084 ± 0.069	$0.52\,^{+0.97}_{-0.22}$ ± 0.10	1

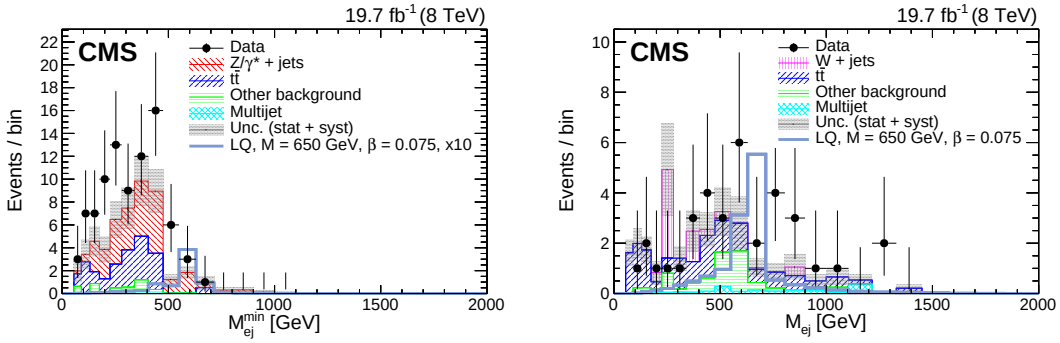

Figure 9: The $M_{\mathrm{ej}}^{\mathrm{min}}$ distribution for the eejj channel (left) and the M_{ej} distribution for the eνjj channel (right) after the selection criteria optimized for a LQ mass of 650 GeV have been applied. The dark shaded region indicates the statistical and systematic uncertainty in the total background prediction. The signal corresponds to a LQ mass of 650 GeV and $\beta = 0.075$. The signal is multiplied by a factor of ten in the left plot. In the case of the eejj analysis, less than one signal event is expected to pass the selection. The horizontal lines on the data points show the variable bin width.

The theoretical cross sections are represented as the central values with a band indicating the sum in quadrature of the PDF uncertainty and the uncertainty associated with the choice of factorization/renormalization scale. The latter is estimated from the observed effect of varying the scale between half and twice the LQ mass.

By comparing the observed upper limit with the theoretical cross section values, first generation scalar LQ with masses less than 1010 (850) GeV are excluded with the assumption that $\beta = 1$ (0.5). This is to be compared with median expected limits of 1030 (890) GeV. Similarly, second generation scalar LQ with masses less than 1080 (760) GeV are excluded with the same assumptions on β, to be compared with median expected limits of 1050 (820) GeV.

The combination of the $\ell\ell$jj and $\ell\nu$jj channels, shown in Fig. 12, excludes LQ masses as a function of β using the intersection of the theoretical cross section central value and the excluded cross section. The combination can improve the mass exclusion reach for values of $\beta < 1$. Using the combined channels, second generation scalar LQ with masses less than 800 GeV are excluded for $\beta = 0.5$, compared with an expected limit of 910 GeV. In the case of first generation LQ, the combination does not lead to a change in the observed limit for $\beta = 0.5$.

The broad excess in the eejj and eνjj channels is most significant for the final selection optimized for a LQ mass of 650 GeV, but has kinematic distributions that do not match those expected for a LQ hypothesis of that mass. Figure 12 shows that the presence of the excess does reduce the exclusion power of the analysis at small values of β ($\lesssim 0.15$) for the selections optimized for LQ masses around 650 GeV. The exclusion limit for this region of the parameter space is dominated by the eνjj channel.

7.3 Additional interpretations

Vector LQ signal samples were simulated with CalcHep at the values of LQ mass detailed in Section 3 for the four scenarios of anomalous couplings described in Section 1. The cross sections for pair production of vector LQs are larger than the ones for the pair production of scalar LQs, therefore we expect a higher reach in the M_{LQ} exclusion limits. The cross sections for vector LQs have been calculated only at the LO level. We assume that the ratios of NLO to

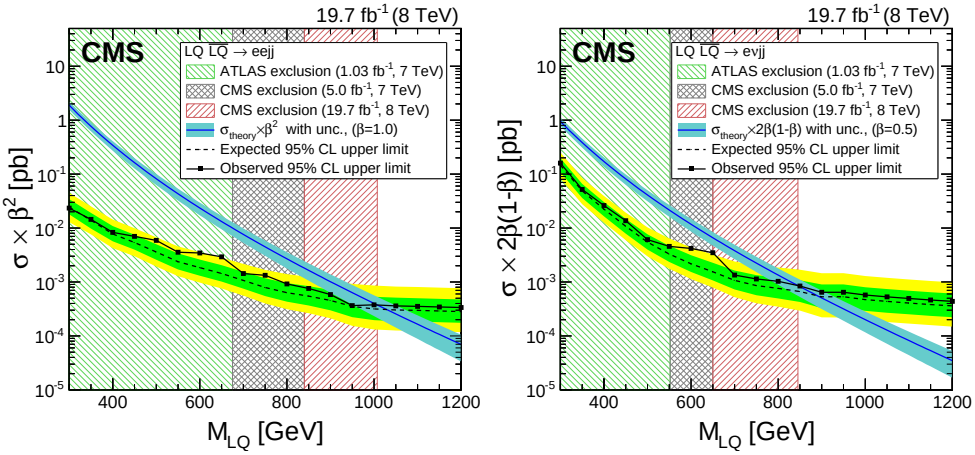

Figure 10: Frame on left (right): the expected and observed upper limits at 95% CL on the LQ pair production cross section times β^2 ($2\beta(1-\beta)$) as a function of the first generation LQ mass obtained with the eejj (eνjj) analysis. The expected limits and uncertainty bands represent the median expected limits and the 68% and 95% confidence intervals. The left shaded regions are excluded by Ref. [77] and the middle shaded regions are excluded by Ref. [24]. The right shaded region is excluded by the analysis presented in this paper. The σ_{theory} curves and their bands represent, respectively, the theoretical scalar LQ pair production cross section and the uncertainties due to the choice of PDF and renormalization/factorization scales.

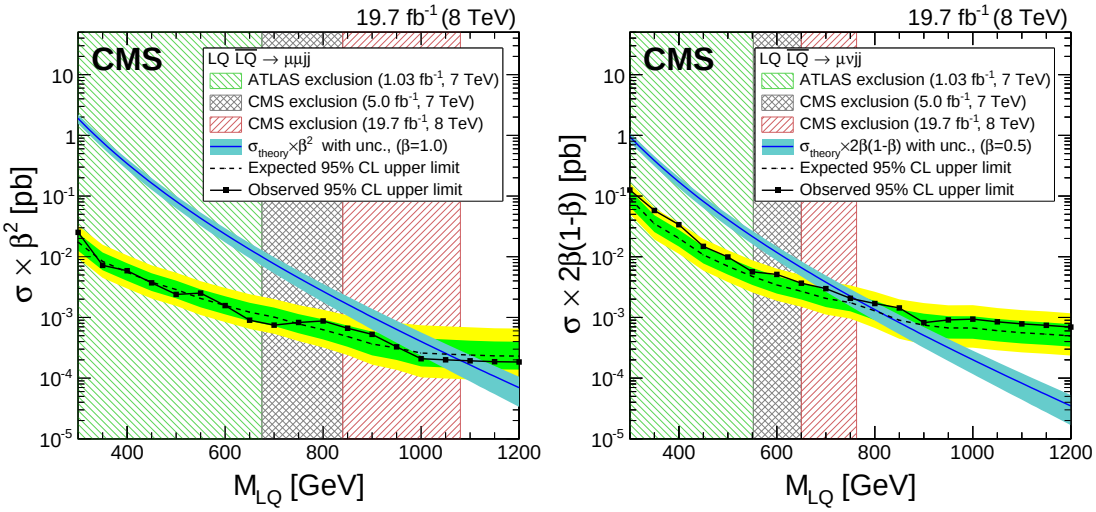

Figure 11: Frame on left (right): the expected and observed upper limits at 95% CL on the LQ pair production cross section times β^2 ($2\beta(1-\beta)$) as a function of the second generation LQ mass obtained with the $\mu\mu$jj ($\mu\nu$jj) analysis. The expected limits and uncertainty bands represent the median expected limits and the 68% and 95% confidence intervals. The left shaded regions are excluded by Ref. [78] and the middle shaded regions are excluded by Ref. [24]. The right shaded region is excluded by the analysis presented in this paper. The σ_{theory} curves and their bands represent, respectively, the theoretical scalar LQ pair production cross section and the uncertainties due to the choice of PDF and renormalization/factorization scales.

LO cross sections for the case of vector LQs are the same as the corresponding ratios for scalar LQs, which vary from 1.62–4.03 over the 300–1800 GeV mass range [19]. In fact, the ratios of

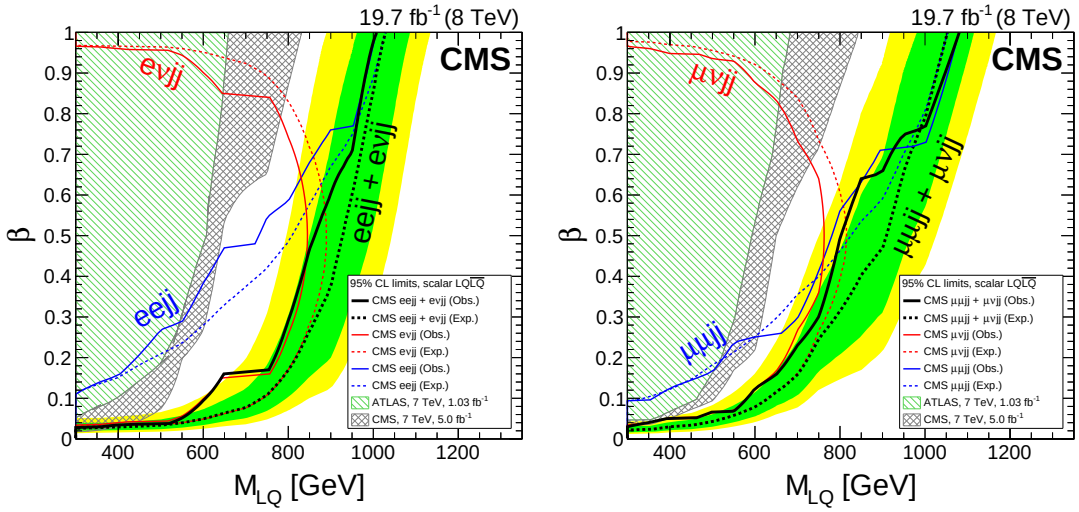

Figure 12: The expected and observed exclusion limits at 95% CL on the first (left) and second (right) generation scalar LQ hypothesis in the β versus LQ mass plane using the central value of signal cross section for the individual $\ell\ell$jj and $\ell\nu$jj channels and their combination. The expected limits and uncertainty bands represent the median expected limits and the 68% and 95% confidence intervals. Solid lines represent the observed limits in each channel, and dashed lines represent the expected limits.

the NLO K-factors for scalar LQ pair production vs. vector LQ pair production are expected to be very similar to the analogous ratios for single LQ production, which have recently been published [79]. Therefore, the limits we obtain by applying the scalar LQ K-factors to the vector LQ LO theoretical curves to obtain predictions for the NLO cross sections are expected to be conservative. The distributions of the kinematic variables for scalar and vector LQs are sufficiently similar that the same event selections and final optimization thresholds can be used for both analyses. It is found that the cross section limits determined using the MC scenario agree within uncertainties with the YM, MM, and AM coupling scenarios. Thus, it is sufficient to overlay the theoretical cross section curves for all vector LQ scenarios with the limit curve calculated using the MC scenario.

Figure 13 shows the experimental limits along with the four theoretical vector LQ cross sections for the eejj (eνjj) channel for $\beta = 1$ (0.5). The experimental results yield a 95% CL upper limit exclusion of masses less than 1470 (1360) GeV assuming YM couplings, 1270 (1160) GeV for the MC couplings scenario, 1660 (1560) GeV for the MM couplings scenario, and 1150 (1050) GeV for the AM scenario. The increased energy and luminosity of the LHC results in considerably improved limits compared to the ones determined by the D0 experiment at the Tevatron [35], which excluded leptoquark masses less than 340 (315) GeV for the case of YM couplings.

Experimental limits along with the four theoretical vector LQ cross sections for the $\mu\mu$jj ($\mu\nu$jj) channel for $\beta = 1$ (0.5) are shown in Fig. 14 on the left (right). In the $\mu\mu$jj ($\mu\nu$jj) channel, the experimental results yield a 95% CL upper limit exclusion of masses less than 1530 (1280) GeV assuming YM couplings, 1330 (1070) GeV for the MC scenario, 1720 (1480) GeV for the MM couplings scenario, and 1200 (980) GeV for the AM couplings scenario. These are the most stringent limits to date on second-generation vector LQ production.

The data have also been compared with an RPV SUSY model described in Ref. [80]. This model predicts light top squarks that decay to a lepton and quark through an R-parity violat-

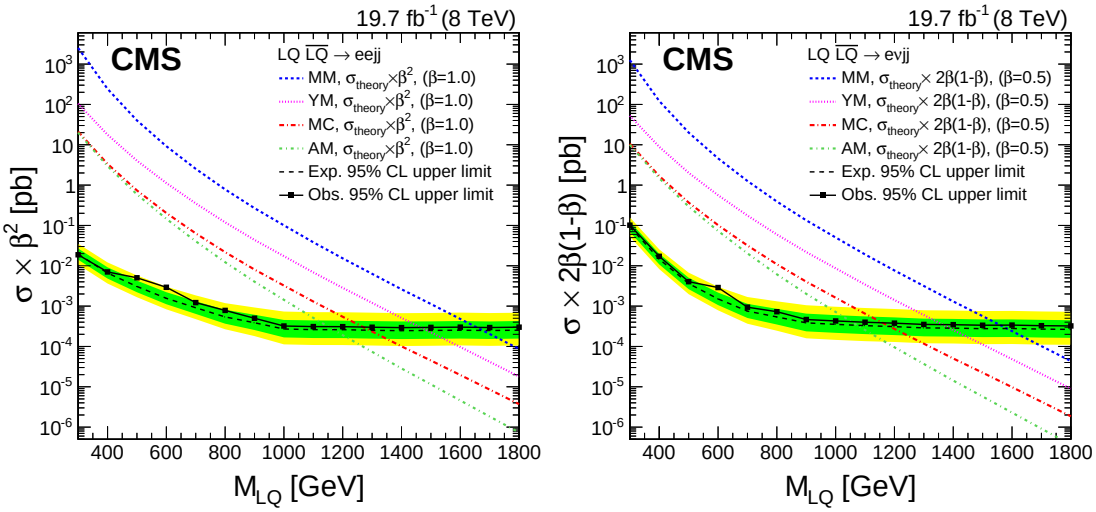

Figure 13: Frame on left (right): the expected and observed upper limits at 95% CL on the vector leptoquark pair production cross section times β^2 ($2\beta(1-\beta)$) as a function of the first generation vector leptoquark mass, obtained with the eejj (eνjj) analysis for the four coupling scenarios (MC, YM, MM, and AM). The expected limits and uncertainty bands represent the median expected limits and the 68% and 95% confidence intervals using the MC scenario. Because of the kinematic similarity between the MC scenario and the other coupling scenarios, cross section limits are found to be the same within the uncertainties.

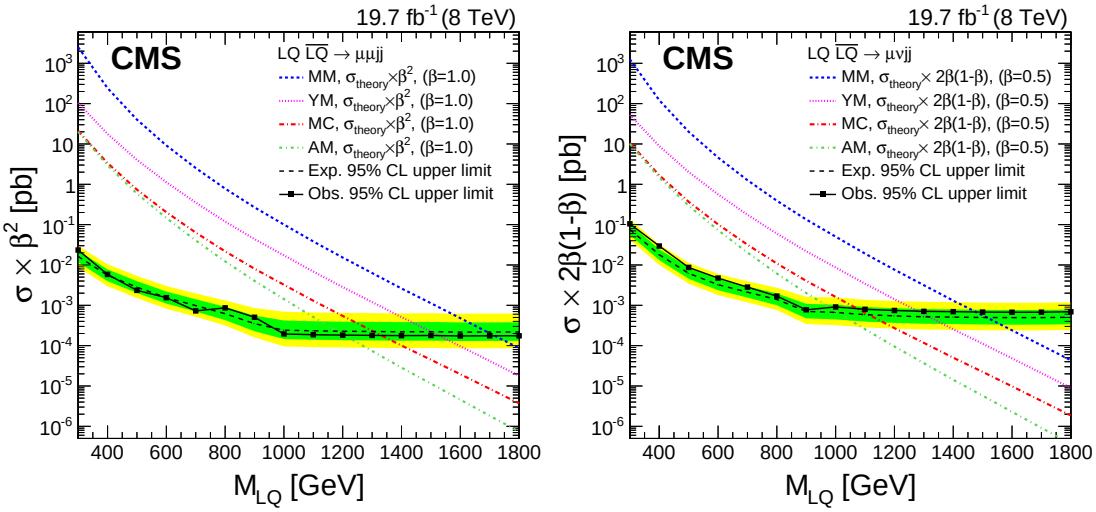

Figure 14: Frame on left (right): the expected and observed upper limits at 95% CL on the vector leptoquark pair production cross section times β^2 ($2\beta(1-\beta)$) as a function of the second generation vector leptoquark mass, obtained with the $\mu\mu$jj ($\mu\nu$jj) analysis for the four coupling scenarios (MC, YM, MM, and AM). The expected limits and uncertainty bands represent the median expected limits and the 68% and 95% confidence intervals using the MC scenario. Because of the kinematic similarity between the MC scenario and the other coupling scenarios, cross section limits are found to be the same within the uncertainties.

ing top squark-lepton-quark vertex (λ') operator. The λ'_{132} (λ'_{232}) operator refers to top squark decay to one electron (muon) and one light-flavor quark. In the case of direct top squark decay, this model is kinematically similar to LQ production, and the limits already described for $\beta = 1$ scalar LQs can be applied simply by scaling for the small difference in production cross sections between top squarks and LQs.

It is interesting to consider the case where top squark decay is mediated by a Higgsino with a mass $M_{\widetilde{H}} = M_{\widetilde{t}} - 100\,\text{GeV}$ with a 100% branching fraction, as shown in Fig. 2. Because of higher jet multiplicity and hence softer kinematic spectra, the optimization selections described in Section 4.1 are shifted such that for a given top squark mass, the selections used correspond to a LQ mass lower by 100 GeV, determined by optimizing the expected limits. The experimental limits along with the theoretical top squark pair production cross sections for the eejj ($\mu\mu$jj) channel are shown in Fig. 15 on the left (right). Assuming this model, the experimental results yield a 95% CL observed upper limit exclusion of top squark masses less than 710 GeV in the first generation λ'_{132} model, compared with a median expected limit of 840 GeV. The second generation λ'_{232} model yields an observed exclusion of top squark masses less than 860 GeV, compared with a median expected limit of 880 GeV. These are the first experimental limits to date on λ'_{132} and λ'_{232} RPV SUSY top squark decays.

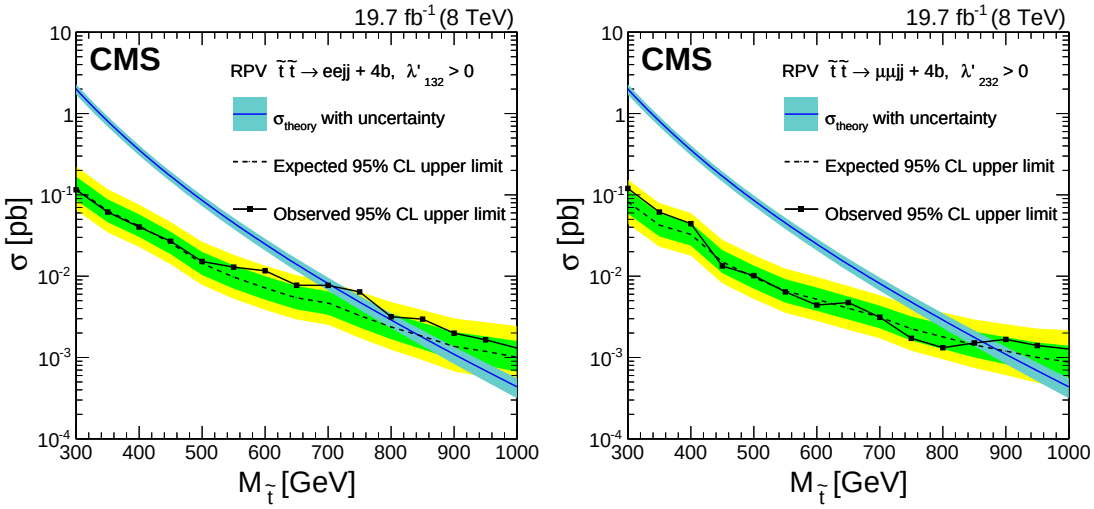

Figure 15: Frame on left (right): the expected and observed upper limits at 95% CL on the top squark pair-production cross section for a Higgsino-mediated RPV SUSY model in the eejj ($\mu\mu$jj) + 4 b quark final state as a function of the top squark mass, obtained with the eejj ($\mu\mu$jj) analysis. The expected limits and uncertainty bands represent the median expected limits and the 68% and 95% confidence intervals. The σ_{theory} curves and their bands represent, respectively, the theoretical top squark pair production cross section and the uncertainties due to the choice of PDF and renormalization/factorization scales.

8 Summary

A search has been conducted for pair production of first- and second-generation scalar leptoquarks in final states with either two electrons (or two muons) and two jets, or with one electron (or muon), significant missing transverse energy, and two jets, using 8 TeV proton-proton collision data corresponding to an integrated luminosity of 19.7 fb^{-1}. The results are also interpreted in the context of models of vector leptoquark pair production and of R-parity violating supersymmetric models with similar final state signatures.

The selection criteria used for all the searches are optimized for each scalar leptoquark signal mass hypothesis. In the first generation eejj (eνjj) channel, a broad 2.3 (2.6) standard deviation excess is observed in the final selection optimized for leptoquarks with a mass of 650 GeV. The excess does not peak in the M_{ej} distributions, as a leptoquark signal would, but does weaken the upper limit that can be set on the production cross section for leptoquark masses of about 650 GeV and values of $\beta \lesssim 0.15$. Limits are placed with 95% CL on first-generation scalar leptoquarks with masses less than 1010 (850) GeV, assuming $\beta = 1.0\ (0.5)$. This is to be compared with the expected 95% CL exclusions of 1030 (890) GeV. In the secondgeneration leptoquark search the number of observed candidates for each mass hypothesis agrees within uncertainties with the number of expected standard model background events. Second-generation scalar leptoquarks are excluded at 95% CL with masses below 1080 (800) GeV for $\beta = 1.0\ (0.5)$. This is to be compared with a median expected limit of 1050 (910) GeV. These results for pair production of scalar leptoquarks are closely comparable to those of Ref. [23].

Limits are set on four coupling scenarios for vector leptoquarks, and for the eejj (eνjj) channel yield 95% CL upper limit exclusions of masses in the range of $1150 - 1660$ $(1050 - 1560)$ GeV. In the $\mu\mu$jj ($\mu\nu$jj) channel, the experimental results yield 95% CL upper limit exclusions of masses in the range of $1200 - 1720$ $(980 - 1480)$ GeV. These represent the most stringent limits on vector LQ production to date.

Limits are also set for top squark production in an R-parity violating supersymmetric model via the λ'_{132} or λ'_{232} operators. For direct top squark decay, the scalar LQ limits can be applied directly. Interpretation is also made in Higgsino-mediated top squark decay, where the experimental results yield a 95% CL observed upper limit exclusion of top squark masses less than 710 GeV in the first generation λ'_{132} model, compared with a median expected limit of 840 GeV. The second generation λ'_{232} model yields an observed exclusion of top squark masses less than 860 GeV, compared with a median expected limit of 880 GeV. These represent the most stringent experimental limits to date on λ'_{132} and λ'_{232} RPV SUSY top squark decays and the first experimental limits on the Higgsino-mediated decays.

Acknowledgments

We congratulate our colleagues in the CERN accelerator departments for the excellent performance of the LHC and thank the technical and administrative staffs at CERN and at other CMS institutes for their contributions to the success of the CMS effort. In addition, we gratefully acknowledge the computing centers and personnel of the Worldwide LHC Computing Grid for delivering so effectively the computing infrastructure essential to our analyses. Finally, we acknowledge the enduring support for the construction and operation of the LHC and the CMS detector provided by the following funding agencies: the Austrian Federal Ministry of Science, Research and Economy and the Austrian Science Fund; the Belgian Fonds de la Recherche Scientifique, and Fonds voor Wetenschappelijk Onderzoek; the Brazilian Funding Agencies (CNPq, CAPES, FAPERJ, and FAPESP); the Bulgarian Ministry of Education and Science; CERN; the Chinese Academy of Sciences, Ministry of Science and Technology, and National Natural Science Foundation of China; the Colombian Funding Agency (COLCIENCIAS); the Croatian Ministry of Science, Education and Sport, and the Croatian Science Foundation; the Research Promotion Foundation, Cyprus; the Ministry of Education and Research, Estonian Research Council via IUT23-4 and IUT23-6 and European Regional Development Fund, Estonia; the Academy of Finland, Finnish Ministry of Education and Culture, and Helsinki Institute of Physics; the Institut National de Physique Nucléaire et de Physique des Particules / CNRS, and Commissariat à l'Énergie Atomique et aux Énergies Alternatives / CEA,

France; the Bundesministerium für Bildung und Forschung, Deutsche Forschungsgemeinschaft, and Helmholtz-Gemeinschaft Deutscher Forschungszentren, Germany; the General Secretariat for Research and Technology, Greece; the National Scientific Research Foundation, and National Innovation Office, Hungary; the Department of Atomic Energy and the Department of Science and Technology, India; the Institute for Studies in Theoretical Physics and Mathematics, Iran; the Science Foundation, Ireland; the Istituto Nazionale di Fisica Nucleare, Italy; the Ministry of Science, ICT and Future Planning, and National Research Foundation (NRF), Republic of Korea; the Lithuanian Academy of Sciences; the Ministry of Education, and University of Malaya (Malaysia); the Mexican Funding Agencies (CINVESTAV, CONACYT, SEP, and UASLP-FAI); the Ministry of Business, Innovation and Employment, New Zealand; the Pakistan Atomic Energy Commission; the Ministry of Science and Higher Education and the National Science Centre, Poland; the Fundação para a Ciência e a Tecnologia, Portugal; JINR, Dubna; the Ministry of Education and Science of the Russian Federation, the Federal Agency of Atomic Energy of the Russian Federation, Russian Academy of Sciences, and the Russian Foundation for Basic Research; the Ministry of Education, Science and Technological Development of Serbia; the Secretaría de Estado de Investigación, Desarrollo e Innovación and Programa Consolider-Ingenio 2010, Spain; the Swiss Funding Agencies (ETH Board, ETH Zurich, PSI, SNF, UniZH, Canton Zurich, and SER); the Ministry of Science and Technology, Taipei; the Thailand Center of Excellence in Physics, the Institute for the Promotion of Teaching Science and Technology of Thailand, Special Task Force for Activating Research and the National Science and Technology Development Agency of Thailand; the Scientific and Technical Research Council of Turkey, and Turkish Atomic Energy Authority; the National Academy of Sciences of Ukraine, and State Fund for Fundamental Researches, Ukraine; the Science and Technology Facilities Council, UK; the US Department of Energy, and the US National Science Foundation.

Individuals have received support from the Marie-Curie program and the European Research Council and EPLANET (European Union); the Leventis Foundation; the A. P. Sloan Foundation; the Alexander von Humboldt Foundation; the Belgian Federal Science Policy Office; the Fonds pour la Formation à la Recherche dans l'Industrie et dans l'Agriculture (FRIA-Belgium); the Agentschap voor Innovatie door Wetenschap en Technologie (IWT-Belgium); the Ministry of Education, Youth and Sports (MEYS) of the Czech Republic; the Council of Science and Industrial Research, India; the HOMING PLUS program of the Foundation for Polish Science, cofinanced from European Union, Regional Development Fund; the OPUS program of the National Science Center (Poland); the Compagnia di San Paolo (Torino); the Consorzio per la Fisica (Trieste); MIUR project 20108T4XTM (Italy); the Thalis and Aristeia programmes cofinanced by EU-ESF and the Greek NSRF; the National Priorities Research Program by Qatar National Research Fund; the Rachadapisek Sompot Fund for Postdoctoral Fellowship, Chulalongkorn University (Thailand); and the Welch Foundation, contract C-1845.

References

[1] J. C. Pati and A. Salam, "Unified Lepton-Hadron Symmetry and a Gauge Theory of the Basic Interactions", *Phys. Rev. D* **8** (1973) 1240, doi:10.1103/PhysRevD.8.1240.

[2] J. C. Pati and A. Salam, "Lepton Number as the Fourth Color", *Phys. Rev. D* **10** (1974) 275, doi:10.1103/PhysRevD.10.275.

[3] H. Georgi and S. Glashow, "Unity of All Elementary-Particle Forces", *Phys. Rev. Lett.* **32** (1974) 438, doi:10.1103/PhysRevLett.32.438.

[4] H. Murayama and T. Yanagida, "A viable SU(5) GUT with light leptoquark bosons", *Mod. Phys. Lett. A* **7** (1992) 147, doi:10.1142/S0217732392000070.

[5] H. Fritzsch and P. Minkowski, "United Interactions of Leptons and Hadrons", *Annals Phys.* **93** (1975) 193, doi:10.1016/0003-4916(75)90211-0.

[6] G. Senjanović and A. Sokorac, "Light lepto-quarks in SO(10)", *Z. Phys. C* **20** (1983) 255, doi:10.1007/BF01574858.

[7] P. H. Frampton and B.-H. Lee, "SU(15) Grand Unification", *Phys. Rev. Lett.* **64** (1990) 619, doi:10.1103/PhysRevLett.64.619.

[8] P. H. Frampton and T. W. Kephart, "Higgs Sector and Proton Decay in SU(15q) Grand Unification", *Phys. Rev. D* **42** (1990) 3892, doi:10.1103/PhysRevD.42.3892.

[9] S. Dimopoulos and L. Susskind, "Mass Without Scalars", *Nucl. Phys. B* **155** (1979) 237, doi:10.1016/0550-3213(81)90304-7.

[10] S. Dimopoulos, "Technicolored Signatures", *Nucl. Phys. B* **168** (1980) 69, doi:10.1016/0550-3213(80)90277-1.

[11] E. Eichten and K. Lane, "Dynamical Breaking of the Weak Interaction Symmetries", *Phys. Lett. B* **90** (1980) 85, doi:10.1016/0370-2693(80)90065-9.

[12] J. L. Hewett and T. G. Rizzo, "Low-energy phenomenology of superstring-inspired E_6 models", *Phys. Lett.* **183** (1989) 193, doi:10.1016/0370-1573(89)90071-9.

[13] B. Schrempp and F. Schrempp, "Light Leptoquarks", *Phys. Lett. B* **153** (1985) 101, doi:10.1016/0370-2693(85)91450-9.

[14] W. Buchmüller, R. Rückl, and D. Wyler, "Leptoquarks in lepton-quark collisions", *Phys. Lett. B* **191** (1987) 442, doi:10.1016/S0370-2693(99)00014-3.

[15] W. Buchmüller and D. Wyler, "Constraints on SU(5)-type leptoquarks", *Phys. Lett. B* **177** (1986) 377, doi:10.1016/0370-2693(86)90771-9.

[16] O. Shanker, "$\pi\ell 2$, K$\ell 3$, and K^0-$\overline{K}^0$ constraints on leptoquarks and supersymmetric particles", *Nucl. Phys. B* **204** (1982) 375, doi:10.1016/0550-3213(82)90196-1.

[17] CMS Collaboration, "Search for single production of scalar leptoquarks in proton-proton collisions at $\sqrt{s} = 8$ TeV", (2015). Submitted to Phys. Rev. D for concurrent publication with this paper.

[18] J. Blumlein, E. Boos, and A. Kryukov, "Leptoquark pair production in hadronic interactions", *Z. Phys. C* **76** (1997) 137, doi:10.1007/s002880050538, arXiv:hep-ph/9610408.

[19] M. Krämer, T. Plehn, M. Spira, and P. M. Zerwas, "Pair production of scalar leptoquarks at the CERN LHC", *Phys. Rev. D* **71** (2005) 057503, doi:10.1103/PhysRevD.71.057503, arXiv:hep-ph/0411038.

[20] H. K. Dreiner, "An introduction to explicit *R*-parity violation", *Pramana* **51** (1998) 123, doi:10.1007/BF02827485.

[21] J. A. Evans and Y. Kats, "LHC coverage of RPV MSSM with light stops", *JHEP* **04** (2013) 028, doi:10.1007/JHEP04(2013)028, arXiv:1209.0764.

[22] A. Belyaev, C. Leroy, R. Mehdiyev, and A. Pukhov, "Leptoquark single and pair production at LHC with CalcHEP/CompHEP in the complete model", *JHEP* **09** (2005) 005, doi:10.1088/1126-6708/2005/09/005, arXiv:hep-ph/0502067.

[23] ATLAS Collaboration, "Searches for scalar leptoquarks in pp collisions at $\sqrt{s} = 8$ TeV with the ATLAS detector", (2015). arXiv:1508.04735.

[24] CMS Collaboration, "Search for pair production of first- and second-generation scalar leptoquarks in pp collisions at $\sqrt{s} = 7$ TeV", *Phys. Rev. D* **86** (2012) 052013, doi:10.1103/PhysRevD.86.052013, arXiv:1207.5406.

[25] CMS Collaboration, "Search for pair production of third-generation scalar leptoquarks and top squarks in proton-proton collisions at $\sqrt{s} = 8$ TeV", *Phys. Lett. B* **739** (2014) 229, doi:10.1016/j.physletb.2014.10.063, arXiv:1408.0806.

[26] ATLAS Collaboration, "Search for third generation scalar leptoquarks in pp collisions at $\sqrt{s} = 7$ TeV with the ATLAS detector", *JHEP* **06** (2013) 033, doi:10.1007/JHEP06(2013)033, arXiv:1303.0526.

[27] H1 Collaboration, "Search for first generation leptoquarks in ep collisions at HERA", *Phys. Lett. B* **704** (2011) 388, doi:10.1016/j.physletb.2011.09.017, arXiv:1107.3716.

[28] ZEUS Collaboration, "Search for first-generation leptoquarks at HERA", *Phys. Rev. D* **86** (2012) 012005, doi:10.1103/PhysRevD.86.012005, arXiv:1205.5179.

[29] D0 Collaboration, "Search for pair production of first-generation leptoquarks in $p\bar{p}$ collisions at $\sqrt{s} = 1.96$ TeV", *Phys. Lett. B* **681** (2009) 224, doi:10.1016/j.physletb.2009.10.016, arXiv:0907.1048.

[30] D0 Collaboration, "Search for pair production of second generation scalar leptoquarks", *Phys. Lett. B* **671** (2009) 224, doi:10.1016/j.physletb.2008.12.017, arXiv:0808.4023.

[31] D0 Collaboration, "Search for first generation leptoquark pair production in the electron + missing energy + jets final state", *Phys. Rev. D* **84** (2011) 071104, doi:10.1103/PhysRevD.84.071104, arXiv:1107.1849.

[32] CDF Collaboration, "Search for first-generation scalar leptoquarks in $p\bar{p}$ collisions at $\sqrt{s} = 1.96$ TeV", *Phys. Rev. D* **72** (2005) 051107, doi:10.1103/PhysRevD.72.051107, arXiv:hep-ex/0506074.

[33] CDF Collaboration, "Search for second-generation scalar leptoquarks in $p\bar{p}$ collisions at $\sqrt{s} = 1.96$ TeV", *Phys. Rev. D* **73** (2006) 051102, doi:10.1103/PhysRevD.73.051102, arXiv:hep-ex/0512055.

[34] CDF Collaboration, "Search for New Physics with a Dijet Plus Missing E_T Signature in $p\bar{p}$ Collisions at $\sqrt{s} = 1.96$ TeV", *Phys. Rev. Lett.* **105** (Sep, 2010) 131801, doi:10.1103/PhysRevLett.105.131801.

[35] *D*0 Collaboration, "Search for first-generation scalar and vector leptoquarks", *Phys. Rev. D* **64** (2001) 092004, doi:10.1103/PhysRevD.64.092004, arXiv:hep-ex/0105072.

[36] D0 Collaboration, "Search for Second Generation Leptoquark Pairs Decaying to $\mu\nu$ + jets in $p\bar{p}$ Collisions at $\sqrt{s} = 1.8$ TeV", *Phys. Rev. Lett.* **83** (1999) 2896, doi:10.1103/PhysRevLett.83.2896, arXiv:hep-ex/9904023.

[37] D0 Collaboration, "Search for second generation leptoquark pairs in $\bar{p}p$ collisions at $\sqrt{s} = 1.8$ TeV", *Phys. Rev. Lett.* **84** (2000) 2088, doi:10.1103/PhysRevLett.84.2088, arXiv:hep-ex/9910040.

[38] CDF Collaboration, "Search for third generation vector leptoquarks in $p\bar{p}$ Collisions at $\sqrt{s} = 1.96$ TeV", *Phys. Rev. D* **77** (2008) 091105, doi:10.1103/PhysRevD.77.091105, arXiv:0706.2832.

[39] CMS Collaboration, "The CMS experiment at the CERN LHC", *JINST* **3** (2008) S08004, doi:10.1088/1748-0221/3/08/S08004.

[40] CMS Collaboration, "Performance of electron reconstruction and selection with the CMS detector in proton-proton collisions at $\sqrt{s} = 8$ TeV", *JINST* **10** (2015), no. 6, P06005, doi:10.1088/1748-0221/10/06/P06005, arXiv:1502.02701.

[41] CMS Collaboration, "CMS Luminosity Based on Pixel Cluster Counting - Summer 2013 Update", CMS Physics Analysis Summary CMS-PAS-LUM-13-001, 2013.

[42] GEANT4 Collaboration, "GEANT4—a simulation toolkit", *Nucl. Instrum. Meth. A* **506** (2003) 250, doi:10.1016/S0168-9002(03)01368-8.

[43] T. Sjöstrand, S. Mrenna, and P. Skands, "PYTHIA 6.4 physics and manual", *JHEP* **05** (2006) 026, doi:10.1088/1126-6708/2006/05/026, arXiv:hep-ph/0603175.

[44] J. Pumplin et al., "New generation of parton distributions with uncertainties from global QCD analysis", *JHEP* **07** (2002) 012, doi:10.1088/1126-6708/2002/07/012, arXiv:hep-ph/0201195.

[45] CMS Collaboration, "Charged particle multiplicities in pp interactions at $\sqrt{s} = 0.9$, 2.36, and 7 TeV", *JHEP* **01** (2010) 079, doi:10.1007/JHEP01(2011)079, arXiv:1011.5531.

[46] A. Belyaev, N. D. Christensen, and A. Pukhov, "CalcHEP 3.4 for collider physics within and beyond the Standard Model", *Comput. Phys. Commun.* **184** (2013) 1729, doi:10.1016/j.cpc.2013.01.014, arXiv:1207.6082.

[47] T. Sjöstrand, S. Mrenna, and P. Z. Skands, "A Brief Introduction to PYTHIA 8.1", *Comput. Phys. Commun.* **178** (2008) 852, doi:10.1016/j.cpc.2008.01.036, arXiv:0710.3820.

[48] J. Alwall et al., "MadGraph 5: going beyond", *JHEP* **06** (2011) 128, doi:10.1007/JHEP06(2011)128, arXiv:1106.0522.

[49] W. Beenakker et al., "Stop production at hadron colliders", *Nucl. Phys. B* **515** (1998) 3, doi:10.1016/S0550-3213(98)00014-5, arXiv:hep-ph/9710451.

[50] W. Beenakker et al., "Supersymmetric top and bottom squark production at hadron colliders", *JHEP* **08** (2010) 098, doi:10.1007/JHEP08(2010)098, arXiv:1006.4771.

[51] W. Beenakker et al., "Squark and Gluino Hadroproduction", *Int. J. Mod. Phys. A* **26** (2011) 2637, doi:10.1142/S0217751X11053560, arXiv:1105.1110.

[52] P. Nason, "A new method for combining NLO QCD with shower Monte Carlo algorithms", *JHEP* **11** (2004) 040, doi:10.1088/1126-6708/2004/11/040, arXiv:hep-ph/0409146.

[53] S. Frixione, P. Nason, and C. Oleari, "Matching NLO QCD computations with parton shower simulations: the POWHEG method", *JHEP* **11** (2007) 070, doi:10.1088/1126-6708/2007/11/070, arXiv:0709.2092.

[54] S. Alioli, P. Nason, C. Oleari, and E. Re, "A general framework for implementing NLO calculations in shower Monte Carlo programs: the POWHEG BOX", *JHEP* **06** (2010) 043, doi:10.1007/JHEP06(2010)043, arXiv:1002.2581.

[55] S. Alioli, P. Nason, C. Oleari, and E. Re, "NLO single-top production matched with shower in POWHEG: s- and t-channel contributions", *JHEP* **09** (2009) 111, doi:10.1088/1126-6708/2009/09/111, arXiv:0907.4076. [Erratum: doi:10.1007/JHEP02(2010)011].

[56] K. Melnikov and F. Petriello, "Electroweak gauge boson production at hadron colliders through $O(\alpha_s^2)$", *Phys. Rev. D* **74** (2006) 114017, doi:10.1103/PhysRevD.74.114017, arXiv:hep-ph/0609070.

[57] J. Campbell, R. K. Ellis, and F. Tramontano, "Single top-quark production and decay at next-to-leading order", *Phys. Rev. D* **70** (2004) 094012, doi:10.1103/PhysRevD.70.094012, arXiv:hep-ph/0408158.

[58] J. Campbell and F. Tramontano, "Next-to-leading order corrections to Wt production and decay", *Nucl. Phys. B* **726** (2005) 109, doi:10.1016/j.nuclphysb.2005.08.015, arXiv:hep-ph/0506289.

[59] J. M. Campbell, R. Frederix, F. Maltoni, and F. Tramontano, "Next-to-Leading-Order Predictions for t-Channel Single-Top Production at Hadron Colliders", *Phys. Rev. Lett.* **102** (2009) 182003, doi:10.1103/PhysRevLett.102.182003, arXiv:0903.0005.

[60] J. M. Campbell, R. K. Ellis, and C. Williams, "Vector boson pair production at the LHC", *JHEP* **07** (2011) 018, doi:10.1007/JHEP07(2011)018, arXiv:1105.0020.

[61] M. Czakon, P. Fiedler, and A. Mitov, "The total top quark pair production cross-section at hadron colliders through O(α_S^4)", *Phys. Rev. Lett.* **110** (2013) 252004, doi:10.1103/PhysRevLett.110.252004, arXiv:1303.6254.

[62] M. Czakon, M. L. Mangano, A. Mitov, and J. Rojo, "Constraints on the gluon PDF from top quark pair production at hadron colliders", *JHEP* **07** (2013) 167, doi:10.1007/JHEP07(2013)167, arXiv:1303.7215.

[63] CMS Collaboration, "Performance of CMS muon reconstruction in pp collision events at $\sqrt{s} = 7$ TeV", *JINST* **7** (2012) 10002, doi:10.1088/1748-0221/7/10/P10002, arXiv:1206.4071.

[64] CMS Collaboration, "Description and performance of track and primary-vertex reconstruction with the CMS tracker", *JINST* **9** (2014) P10009, doi:10.1088/1748-0221/9/10/P10009, arXiv:1405.6569.

[65] CMS Collaboration, "Particle–Flow Event Reconstruction in CMS and Performance for Jets, Taus, and $E_{\mathrm{T}}^{\mathrm{miss}}$", CMS Physics Analysis Summary CMS-PAS-PFT-09-001, 2009.

[66] CMS Collaboration, "Commissioning of the Particle-flow Event Reconstruction with the first LHC collisions recorded in the CMS detector", CMS Physics Analysis Summary CMS-PAS-PFT-10-001, 2010.

[67] M. Cacciari, G. P. Salam, and G. Soyez, "The anti-k_{T} jet clustering algorithm", *JHEP* **04** (2008) 063, doi:10.1088/1126-6708/2008/04/063, arXiv:0802.1189.

[68] M. Cacciari, G. P. Salam, and G. Soyez, "FastJet user manual", *Eur. Phys. J. C* **72** (2012) 1896, doi:10.1140/epjc/s10052-012-1896-2, arXiv:1111.6097.

[69] CMS Collaboration, "Determination of jet energy calibration and transverse momentum resolution in CMS", *JINST* **6** (2011) 11002, doi:10.1088/1748-0221/6/11/P11002, arXiv:1107.4277.

[70] CMS Collaboration, "Search for physics beyond the standard model in dilepton mass spectra in proton-proton collisions at $\sqrt{s} = 8$ TeV", *JHEP* **04** (2015) 025, doi:10.1007/JHEP04(2015)025, arXiv:1412.6302.

[71] S. Alekhin and otherss, "The PDF4LHC Working Group Interim Report", (2011). arXiv:1101.0536.

[72] M. Botje et al., "The PDF4LHC Working Group Interim Recommendations", (2011). arXiv:1101.0538.

[73] CMS Collaboration, "Identification of b-quark jets with the CMS experiment", *JINST* **8** (2013) P04013, doi:10.1088/1748-0221/8/04/P04013, arXiv:1211.4462.

[74] CMS Collaboration, "Search for heavy neutrinos and W bosons with right-handed couplings in proton-proton collisions at $\sqrt{s} = 8$ TeV", *Eur. Phys. J. C* **74** (2014) 3149, doi:10.1140/epjc/s10052-014-3149-z, arXiv:1407.3683.

[75] T. Junk, "Confidence level computation for combining searches with small statistics", *Nucl. Instrum. Meth. A* **434** (1999) 435, doi:10.1016/S0168-9002(99)00498-2, arXiv:hep-ex/9902006.

[76] A. L. Read, "Presentation of search results: the CL_s technique", *J. Phys. G* **28** (2002) 2693, doi:10.1088/0954-3899/28/10/313.

[77] ATLAS Collaboration, "Search for first generation scalar leptoquarks in pp collisions at $\sqrt{s} = 7$ TeV with the ATLAS detector", *Phys. Lett. B* **709** (2012) 158, doi:10.1016/j.physletb.2012.02.004, arXiv:1112.4828. [Erratum: doi:10.1016/j.physletb.2012.03.023].

[78] ATLAS Collaboration, "Search for second generation scalar leptoquarks in pp collisions at $\sqrt{s} = 7$ TeV with the ATLAS detector", *Eur. Phys. J. C* **72** (2012) 2151, doi:10.1140/epjc/s10052-012-2151-6, arXiv:1203.3172.

[79] J. B. Hammett and D. A. Ross, "NLO leptoquark production and decay: the narrow-width approximation and beyond", *JHEP* **07** (2015) 148, doi:10.1007/JHEP07(2015)148, arXiv:1501.06719.

[80] J. A. Evans and Y. Kats, "LHC searches examined via the RPV MSSM", in *Proceedings of the EPS Conference on HEP (EPS-HEP) 2013*, p. 287. SISSA, 2013. arXiv:1311.0890. PoS(EPS-HEP 2013)287.

A The CMS Collaboration

Yerevan Physics Institute, Yerevan, Armenia
V. Khachatryan, A.M. Sirunyan, A. Tumasyan

Institut für Hochenergiephysik der OeAW, Wien, Austria
W. Adam, E. Asilar, T. Bergauer, J. Brandstetter, E. Brondolin, M. Dragicevic, J. Erö, M. Flechl, M. Friedl, R. Frühwirth[1], V.M. Ghete, C. Hartl, N. Hörmann, J. Hrubec, M. Jeitler[1], V. Knünz, A. König, M. Krammer[1], I. Krätschmer, D. Liko, T. Matsushita, I. Mikulec, D. Rabady[2], B. Rahbaran, H. Rohringer, J. Schieck[1], R. Schöfbeck, J. Strauss, W. Treberer-Treberspurg, W. Waltenberger, C.-E. Wulz[1]

National Centre for Particle and High Energy Physics, Minsk, Belarus
V. Mossolov, N. Shumeiko, J. Suarez Gonzalez

Universiteit Antwerpen, Antwerpen, Belgium
S. Alderweireldt, T. Cornelis, E.A. De Wolf, X. Janssen, A. Knutsson, J. Lauwers, S. Luyckx, S. Ochesanu, R. Rougny, M. Van De Klundert, H. Van Haevermaet, P. Van Mechelen, N. Van Remortel, A. Van Spilbeeck

Vrije Universiteit Brussel, Brussel, Belgium
S. Abu Zeid, F. Blekman, J. D'Hondt, N. Daci, I. De Bruyn, K. Deroover, N. Heracleous, J. Keaveney, S. Lowette, L. Moreels, A. Olbrechts, Q. Python, D. Strom, S. Tavernier, W. Van Doninck, P. Van Mulders, G.P. Van Onsem, I. Van Parijs

Université Libre de Bruxelles, Bruxelles, Belgium
P. Barria, C. Caillol, B. Clerbaux, G. De Lentdecker, H. Delannoy, D. Dobur, G. Fasanella, L. Favart, A.P.R. Gay, A. Grebenyuk, T. Lenzi, A. Léonard, T. Maerschalk, A. Marinov, A. Mohammadi, L. Perniè, A. Randle-conde, T. Reis, T. Seva, C. Vander Velde, P. Vanlaer, R. Yonamine, F. Zenoni, F. Zhang[3]

Ghent University, Ghent, Belgium
K. Beernaert, L. Benucci, A. Cimmino, S. Crucy, A. Fagot, G. Garcia, M. Gul, J. Mccartin, A.A. Ocampo Rios, D. Poyraz, D. Ryckbosch, S. Salva, M. Sigamani, N. Strobbe, M. Tytgat, W. Van Driessche, E. Yazgan, N. Zaganidis

Université Catholique de Louvain, Louvain-la-Neuve, Belgium
S. Basegmez, C. Beluffi[4], O. Bondu, G. Bruno, R. Castello, A. Caudron, L. Ceard, G.G. Da Silveira, C. Delaere, D. Favart, L. Forthomme, A. Giammanco[5], J. Hollar, A. Jafari, P. Jez, M. Komm, V. Lemaitre, A. Mertens, C. Nuttens, L. Perrini, A. Pin, K. Piotrzkowski, A. Popov[6], L. Quertenmont, M. Selvaggi, M. Vidal Marono

Université de Mons, Mons, Belgium
N. Beliy, G.H. Hammad

Centro Brasileiro de Pesquisas Fisicas, Rio de Janeiro, Brazil
W.L. Aldá Júnior, G.A. Alves, L. Brito, M. Correa Martins Junior, T. Dos Reis Martins, C. Hensel, C. Mora Herrera, A. Moraes, M.E. Pol, P. Rebello Teles

Universidade do Estado do Rio de Janeiro, Rio de Janeiro, Brazil
E. Belchior Batista Das Chagas, W. Carvalho, J. Chinellato[7], A. Custódio, E.M. Da Costa, D. De Jesus Damiao, C. De Oliveira Martins, S. Fonseca De Souza, L.M. Huertas Guativa, H. Malbouisson, D. Matos Figueiredo, L. Mundim, H. Nogima, W.L. Prado Da Silva, A. Santoro, A. Sznajder, E.J. Tonelli Manganote[7], A. Vilela Pereira

Universidade Estadual Paulista [a], Universidade Federal do ABC [b], São Paulo, Brazil
S. Ahuja[a], C.A. Bernardes[b], A. De Souza Santos[b], S. Dogra[a], T.R. Fernandez Perez Tomei[a], E.M. Gregores[b], P.G. Mercadante[b], C.S. Moon[a,8], S.F. Novaes[a], Sandra S. Padula[a], D. Romero Abad, J.C. Ruiz Vargas

Institute for Nuclear Research and Nuclear Energy, Sofia, Bulgaria
A. Aleksandrov, V. Genchev†, R. Hadjiiska, P. Iaydjiev, S. Piperov, M. Rodozov, S. Stoykova, G. Sultanov, M. Vutova

University of Sofia, Sofia, Bulgaria
A. Dimitrov, I. Glushkov, L. Litov, B. Pavlov, P. Petkov

Institute of High Energy Physics, Beijing, China
M. Ahmad, J.G. Bian, G.M. Chen, H.S. Chen, M. Chen, T. Cheng, R. Du, C.H. Jiang, R. Plestina[9], F. Romeo, S.M. Shaheen, J. Tao, C. Wang, Z. Wang, H. Zhang

State Key Laboratory of Nuclear Physics and Technology, Peking University, Beijing, China
C. Asawatangtrakuldee, Y. Ban, Q. Li, S. Liu, Y. Mao, S.J. Qian, D. Wang, Z. Xu, W. Zou

Universidad de Los Andes, Bogota, Colombia
C. Avila, A. Cabrera, L.F. Chaparro Sierra, C. Florez, J.P. Gomez, B. Gomez Moreno, J.C. Sanabria

University of Split, Faculty of Electrical Engineering, Mechanical Engineering and Naval Architecture, Split, Croatia
N. Godinovic, D. Lelas, D. Polic, I. Puljak

University of Split, Faculty of Science, Split, Croatia
Z. Antunovic, M. Kovac

Institute Rudjer Boskovic, Zagreb, Croatia
V. Brigljevic, K. Kadija, J. Luetic, L. Sudic

University of Cyprus, Nicosia, Cyprus
A. Attikis, G. Mavromanolakis, J. Mousa, C. Nicolaou, F. Ptochos, P.A. Razis, H. Rykaczewski

Charles University, Prague, Czech Republic
M. Bodlak, M. Finger[10], M. Finger Jr.[10]

Academy of Scientific Research and Technology of the Arab Republic of Egypt, Egyptian Network of High Energy Physics, Cairo, Egypt
S. Aly[11], Y. Assran[12], S. Elgammal[13], A. Ellithi Kamel[14], A. Lotfy[15], M.A. Mahmoud[15], A. Radi[13,16], A. Sayed[16,13]

National Institute of Chemical Physics and Biophysics, Tallinn, Estonia
B. Calpas, M. Kadastik, M. Murumaa, M. Raidal, A. Tiko, C. Veelken

Department of Physics, University of Helsinki, Helsinki, Finland
P. Eerola, J. Pekkanen, M. Voutilainen

Helsinki Institute of Physics, Helsinki, Finland
J. Härkönen, V. Karimäki, R. Kinnunen, T. Lampén, K. Lassila-Perini, S. Lehti, T. Lindén, P. Luukka, T. Mäenpää, T. Peltola, E. Tuominen, J. Tuominiemi, E. Tuovinen, L. Wendland

Lappeenranta University of Technology, Lappeenranta, Finland
J. Talvitie, T. Tuuva

DSM/IRFU, CEA/Saclay, Gif-sur-Yvette, France
M. Besancon, F. Couderc, M. Dejardin, D. Denegri, B. Fabbro, J.L. Faure, C. Favaro, F. Ferri, S. Ganjour, A. Givernaud, P. Gras, G. Hamel de Monchenault, P. Jarry, E. Locci, M. Machet, J. Malcles, J. Rander, A. Rosowsky, M. Titov, A. Zghiche

Laboratoire Leprince-Ringuet, Ecole Polytechnique, IN2P3-CNRS, Palaiseau, France
S. Baffioni, F. Beaudette, P. Busson, L. Cadamuro, E. Chapon, C. Charlot, T. Dahms, O. Davignon, N. Filipovic, A. Florent, R. Granier de Cassagnac, S. Lisniak, L. Mastrolorenzo, P. Miné, I.N. Naranjo, M. Nguyen, C. Ochando, G. Ortona, P. Paganini, S. Regnard, R. Salerno, J.B. Sauvan, Y. Sirois, T. Strebler, Y. Yilmaz, A. Zabi

Institut Pluridisciplinaire Hubert Curien, Université de Strasbourg, Université de Haute Alsace Mulhouse, CNRS/IN2P3, Strasbourg, France
J.-L. Agram[17], J. Andrea, A. Aubin, D. Bloch, J.-M. Brom, M. Buttignol, E.C. Chabert, N. Chanon, C. Collard, E. Conte[17], X. Coubez, J.-C. Fontaine[17], D. Gelé, U. Goerlach, C. Goetzmann, A.-C. Le Bihan, J.A. Merlin[2], K. Skovpen, P. Van Hove

Centre de Calcul de l'Institut National de Physique Nucleaire et de Physique des Particules, CNRS/IN2P3, Villeurbanne, France
S. Gadrat

Université de Lyon, Université Claude Bernard Lyon 1, CNRS-IN2P3, Institut de Physique Nucléaire de Lyon, Villeurbanne, France
S. Beauceron, C. Bernet, G. Boudoul, E. Bouvier, S. Brochet, C.A. Carrillo Montoya, J. Chasserat, R. Chierici, D. Contardo, B. Courbon, P. Depasse, H. El Mamouni, J. Fan, J. Fay, S. Gascon, M. Gouzevitch, B. Ille, I.B. Laktineh, M. Lethuillier, L. Mirabito, A.L. Pequegnot, S. Perries, J.D. Ruiz Alvarez, D. Sabes, L. Sgandurra, V. Sordini, M. Vander Donckt, P. Verdier, S. Viret, H. Xiao

Georgian Technical University, Tbilisi, Georgia
T. Toriashvili[18]

Tbilisi State University, Tbilisi, Georgia
D. Lomidze

RWTH Aachen University, I. Physikalisches Institut, Aachen, Germany
C. Autermann, S. Beranek, M. Edelhoff, L. Feld, A. Heister, M.K. Kiesel, K. Klein, M. Lipinski, A. Ostapchuk, M. Preuten, F. Raupach, J. Sammet, S. Schael, J.F. Schulte, T. Verlage, H. Weber, B. Wittmer, V. Zhukov[6]

RWTH Aachen University, III. Physikalisches Institut A, Aachen, Germany
M. Ata, M. Brodski, E. Dietz-Laursonn, D. Duchardt, M. Endres, M. Erdmann, S. Erdweg, T. Esch, R. Fischer, A. Güth, T. Hebbeker, C. Heidemann, K. Hoepfner, D. Klingebiel, S. Knutzen, P. Kreuzer, M. Merschmeyer, A. Meyer, P. Millet, M. Olschewski, K. Padeken, P. Papacz, T. Pook, M. Radziej, H. Reithler, M. Rieger, F. Scheuch, L. Sonnenschein, D. Teyssier, S. Thüer

RWTH Aachen University, III. Physikalisches Institut B, Aachen, Germany
V. Cherepanov, Y. Erdogan, G. Flügge, H. Geenen, M. Geisler, F. Hoehle, B. Kargoll, T. Kress, Y. Kuessel, A. Künsken, J. Lingemann[2], A. Nehrkorn, A. Nowack, I.M. Nugent, C. Pistone, O. Pooth, A. Stahl

Deutsches Elektronen-Synchrotron, Hamburg, Germany
M. Aldaya Martin, I. Asin, N. Bartosik, O. Behnke, U. Behrens, A.J. Bell, K. Borras,

A. Burgmeier, A. Cakir, L. Calligaris, A. Campbell, S. Choudhury, F. Costanza, C. Diez Pardos, G. Dolinska, S. Dooling, T. Dorland, G. Eckerlin, D. Eckstein, T. Eichhorn, G. Flucke, E. Gallo, J. Garay Garcia, A. Geiser, A. Gizhko, P. Gunnellini, J. Hauk, M. Hempel[19], H. Jung, A. Kalogeropoulos, O. Karacheban[19], M. Kasemann, P. Katsas, J. Kieseler, C. Kleinwort, I. Korol, W. Lange, J. Leonard, K. Lipka, A. Lobanov, W. Lohmann[19], R. Mankel, I. Marfin[19], I.-A. Melzer-Pellmann, A.B. Meyer, G. Mittag, J. Mnich, A. Mussgiller, S. Naumann-Emme, A. Nayak, E. Ntomari, H. Perrey, D. Pitzl, R. Placakyte, A. Raspereza, P.M. Ribeiro Cipriano, B. Roland, M.Ö. Sahin, P. Saxena, T. Schoerner-Sadenius, M. Schröder, C. Seitz, S. Spannagel, K.D. Trippkewitz, C. Wissing

University of Hamburg, Hamburg, Germany
V. Blobel, M. Centis Vignali, A.R. Draeger, J. Erfle, E. Garutti, K. Goebel, D. Gonzalez, M. Görner, J. Haller, M. Hoffmann, R.S. Höing, A. Junkes, R. Klanner, R. Kogler, T. Lapsien, T. Lenz, I. Marchesini, D. Marconi, D. Nowatschin, J. Ott, F. Pantaleo[2], T. Peiffer, A. Perieanu, N. Pietsch, J. Poehlsen, D. Rathjens, C. Sander, H. Schettler, P. Schleper, E. Schlieckau, A. Schmidt, J. Schwandt, M. Seidel, V. Sola, H. Stadie, G. Steinbrück, H. Tholen, D. Troendle, E. Usai, L. Vanelderen, A. Vanhoefer

Institut für Experimentelle Kernphysik, Karlsruhe, Germany
M. Akbiyik, C. Barth, C. Baus, J. Berger, C. Böser, E. Butz, T. Chwalek, F. Colombo, W. De Boer, A. Descroix, A. Dierlamm, M. Feindt, F. Frensch, M. Giffels, A. Gilbert, F. Hartmann[2], U. Husemann, F. Kassel[2], I. Katkov[6], A. Kornmayer[2], P. Lobelle Pardo, M.U. Mozer, T. Müller, Th. Müller, M. Plagge, G. Quast, K. Rabbertz, S. Röcker, F. Roscher, H.J. Simonis, F.M. Stober, R. Ulrich, J. Wagner-Kuhr, S. Wayand, T. Weiler, C. Wöhrmann, R. Wolf

Institute of Nuclear and Particle Physics (INPP), NCSR Demokritos, Aghia Paraskevi, Greece
G. Anagnostou, G. Daskalakis, T. Geralis, V.A. Giakoumopoulou, A. Kyriakis, D. Loukas, A. Markou, A. Psallidas, I. Topsis-Giotis

University of Athens, Athens, Greece
A. Agapitos, S. Kesisoglou, A. Panagiotou, N. Saoulidou, E. Tziaferi

University of Ioánnina, Ioánnina, Greece
I. Evangelou, G. Flouris, C. Foudas, P. Kokkas, N. Loukas, N. Manthos, I. Papadopoulos, E. Paradas, J. Strologas

Wigner Research Centre for Physics, Budapest, Hungary
G. Bencze, C. Hajdu, A. Hazi, P. Hidas, D. Horvath[20], F. Sikler, V. Veszpremi, G. Vesztergombi[21], A.J. Zsigmond

Institute of Nuclear Research ATOMKI, Debrecen, Hungary
N. Beni, S. Czellar, J. Karancsi[22], J. Molnar, Z. Szillasi

University of Debrecen, Debrecen, Hungary
M. Bartók[23], A. Makovec, P. Raics, Z.L. Trocsanyi, B. Ujvari

National Institute of Science Education and Research, Bhubaneswar, India
P. Mal, K. Mandal, N. Sahoo, S.K. Swain

Panjab University, Chandigarh, India
S. Bansal, S.B. Beri, V. Bhatnagar, R. Chawla, R. Gupta, U.Bhawandeep, A.K. Kalsi, A. Kaur, M. Kaur, R. Kumar, A. Mehta, M. Mittal, N. Nishu, J.B. Singh, G. Walia

University of Delhi, Delhi, India
Ashok Kumar, Arun Kumar, A. Bhardwaj, B.C. Choudhary, R.B. Garg, A. Kumar, S. Malhotra, M. Naimuddin, K. Ranjan, R. Sharma, V. Sharma

Saha Institute of Nuclear Physics, Kolkata, India
S. Banerjee, S. Bhattacharya, K. Chatterjee, S. Dey, S. Dutta, Sa. Jain, Sh. Jain, R. Khurana, N. Majumdar, A. Modak, K. Mondal, S. Mukherjee, S. Mukhopadhyay, A. Roy, D. Roy, S. Roy Chowdhury, S. Sarkar, M. Sharan

Bhabha Atomic Research Centre, Mumbai, India
A. Abdulsalam, R. Chudasama, D. Dutta, V. Jha, V. Kumar, A.K. Mohanty[2], L.M. Pant, P. Shukla, A. Topkar

Tata Institute of Fundamental Research, Mumbai, India
T. Aziz, S. Banerjee, S. Bhowmik[24], R.M. Chatterjee, R.K. Dewanjee, S. Dugad, S. Ganguly, S. Ghosh, M. Guchait, A. Gurtu[25], G. Kole, S. Kumar, B. Mahakud, M. Maity[24], G. Majumder, K. Mazumdar, S. Mitra, G.B. Mohanty, B. Parida, T. Sarkar[24], K. Sudhakar, N. Sur, B. Sutar, N. Wickramage[26]

Indian Institute of Science Education and Research (IISER), Pune, India
S. Sharma

Institute for Research in Fundamental Sciences (IPM), Tehran, Iran
H. Bakhshiansohi, H. Behnamian, S.M. Etesami[27], A. Fahim[28], R. Goldouzian, M. Khakzad, M. Mohammadi Najafabadi, M. Naseri, S. Paktinat Mehdiabadi, F. Rezaei Hosseinabadi, B. Safarzadeh[29], M. Zeinali

University College Dublin, Dublin, Ireland
M. Felcini, M. Grunewald

INFN Sezione di Bari [a], Università di Bari [b], Politecnico di Bari [c], Bari, Italy
M. Abbrescia[a,b], C. Calabria[a,b], C. Caputo[a,b], S.S. Chhibra[a,b], A. Colaleo[a], D. Creanza[a,c], L. Cristella[a,b], N. De Filippis[a,c], M. De Palma[a,b], L. Fiore[a], G. Iaselli[a,c], G. Maggi[a,c], M. Maggi[a], G. Miniello[a,b], S. My[a,c], S. Nuzzo[a,b], A. Pompili[a,b], G. Pugliese[a,c], R. Radogna[a,b], A. Ranieri[a], G. Selvaggi[a,b], L. Silvestris[a,2], R. Venditti[a,b], P. Verwilligen[a]

INFN Sezione di Bologna [a], Università di Bologna [b], Bologna, Italy
G. Abbiendi[a], C. Battilana[2], A.C. Benvenuti[a], D. Bonacorsi[a,b], S. Braibant-Giacomelli[a,b], L. Brigliadori[a,b], R. Campanini[a,b], P. Capiluppi[a,b], A. Castro[a,b], F.R. Cavallo[a], G. Codispoti[a,b], M. Cuffiani[a,b], G.M. Dallavalle[a], F. Fabbri[a], A. Fanfani[a,b], D. Fasanella[a,b], P. Giacomelli[a], C. Grandi[a], L. Guiducci[a,b], S. Marcellini[a], G. Masetti[a], A. Montanari[a], F.L. Navarria[a,b], A. Perrotta[a], A.M. Rossi[a,b], T. Rovelli[a,b], G.P. Siroli[a,b], N. Tosi[a,b], R. Travaglini[a,b]

INFN Sezione di Catania [a], Università di Catania [b], CSFNSM [c], Catania, Italy
G. Cappello[a], M. Chiorboli[a,b], S. Costa[a,b], F. Giordano[a,c], R. Potenza[a,b], A. Tricomi[a,b], C. Tuve[a,b]

INFN Sezione di Firenze [a], Università di Firenze [b], Firenze, Italy
G. Barbagli[a], V. Ciulli[a,b], C. Civinini[a], R. D'Alessandro[a,b], E. Focardi[a,b], S. Gonzi[a,b], V. Gori[a,b], P. Lenzi[a,b], M. Meschini[a], S. Paoletti[a], G. Sguazzoni[a], A. Tropiano[a,b], L. Viliani[a,b]

INFN Laboratori Nazionali di Frascati, Frascati, Italy
L. Benussi, S. Bianco, F. Fabbri, D. Piccolo

INFN Sezione di Genova [a], Università di Genova [b], Genova, Italy
V. Calvelli[a,b], F. Ferro[a], M. Lo Vetere[a,b], E. Robutti[a], S. Tosi[a,b]

INFN Sezione di Milano-Bicocca [a], Università di Milano-Bicocca [b], Milano, Italy
M.E. Dinardo[a,b], S. Fiorendi[a,b], S. Gennai[a], R. Gerosa[a,b], A. Ghezzi[a,b], P. Govoni[a,b], S. Malvezzi[a], R.A. Manzoni[a,b], B. Marzocchi[a,b,2], D. Menasce[a], L. Moroni[a], M. Paganoni[a,b], D. Pedrini[a], S. Ragazzi[a,b], N. Redaelli[a], T. Tabarelli de Fatis[a,b]

INFN Sezione di Napoli [a], Università di Napoli 'Federico II' [b], Napoli, Italy, Università della Basilicata [c], Potenza, Italy, Università G. Marconi [d], Roma, Italy
S. Buontempo[a], N. Cavallo[a,c], S. Di Guida[a,d,2], M. Esposito[a,b], F. Fabozzi[a,c], A.O.M. Iorio[a,b], G. Lanza[a], L. Lista[a], S. Meola[a,d,2], M. Merola[a], P. Paolucci[a,2], C. Sciacca[a,b], F. Thyssen

INFN Sezione di Padova [a], Università di Padova [b], Padova, Italy, Università di Trento [c], Trento, Italy
P. Azzi[a,2], N. Bacchetta[a], D. Bisello[a,b], A. Boletti[a,b], A. Branca[a,b], R. Carlin[a,b], A. Carvalho Antunes De Oliveira[a,b], P. Checchia[a], M. Dall'Osso[a,b,2], T. Dorigo[a], U. Dosselli[a], F. Gasparini[a,b], U. Gasparini[a,b], F. Gonella[a], A. Gozzelino[a], K. Kanishchev[a,c], S. Lacaprara[a], M. Margoni[a,b], A.T. Meneguzzo[a,b], J. Pazzini[a,b], N. Pozzobon[a,b], P. Ronchese[a,b], F. Simonetto[a,b], E. Torassa[a], M. Tosi[a,b], M. Zanetti, P. Zotto[a,b], A. Zucchetta[a,b,2]

INFN Sezione di Pavia [a], Università di Pavia [b], Pavia, Italy
A. Braghieri[a], A. Magnani[a], S.P. Ratti[a,b], V. Re[a], C. Riccardi[a,b], P. Salvini[a], I. Vai[a], P. Vitulo[a,b]

INFN Sezione di Perugia [a], Università di Perugia [b], Perugia, Italy
L. Alunni Solestizi[a,b], M. Biasini[a,b], G.M. Bilei[a], D. Ciangottini[a,b,2], L. Fanò[a,b], P. Lariccia[a,b], G. Mantovani[a,b], M. Menichelli[a], A. Saha[a], A. Santocchia[a,b], A. Spiezia[a,b]

INFN Sezione di Pisa [a], Università di Pisa [b], Scuola Normale Superiore di Pisa [c], Pisa, Italy
K. Androsov[a,30], P. Azzurri[a], G. Bagliesi[a], J. Bernardini[a], T. Boccali[a], G. Broccolo[a,c], R. Castaldi[a], M.A. Ciocci[a,30], R. Dell'Orso[a], S. Donato[a,c,2], G. Fedi, L. Foà[a,c†], A. Giassi[a], M.T. Grippo[a,30], F. Ligabue[a,c], T. Lomtadze[a], L. Martini[a,b], A. Messineo[a,b], F. Palla[a], A. Rizzi[a,b], A. Savoy-Navarro[a,31], A.T. Serban[a], P. Spagnolo[a], P. Squillacioti[a,30], R. Tenchini[a], G. Tonelli[a,b], A. Venturi[a], P.G. Verdini[a]

INFN Sezione di Roma [a], Università di Roma [b], Roma, Italy
L. Barone[a,b], F. Cavallari[a], G. D'imperio[a,b,2], D. Del Re[a,b], M. Diemoz[a], S. Gelli[a,b], C. Jorda[a], E. Longo[a,b], F. Margaroli[a,b], P. Meridiani[a], F. Micheli[a,b], G. Organtini[a,b], R. Paramatti[a], F. Preiato[a,b], S. Rahatlou[a,b], C. Rovelli[a], F. Santanastasio[a,b], P. Traczyk[a,b,2]

INFN Sezione di Torino [a], Università di Torino [b], Torino, Italy, Università del Piemonte Orientale [c], Novara, Italy
N. Amapane[a,b], R. Arcidiacono[a,c,2], S. Argiro[a,b], M. Arneodo[a,c], R. Bellan[a,b], C. Biino[a], N. Cartiglia[a], M. Costa[a,b], R. Covarelli[a,b], D. Dattola[a], A. Degano[a,b], G. Dellacasa[a], N. Demaria[a], L. Finco[a,b,2], C. Mariotti[a], S. Maselli[a], E. Migliore[a,b], V. Monaco[a,b], E. Monteil[a,b], M. Musich[a], M.M. Obertino[a,b], L. Pacher[a,b], N. Pastrone[a], M. Pelliccioni[a], G.L. Pinna Angioni[a,b], F. Ravera[a,b], A. Romero[a,b], M. Ruspa[a,c], R. Sacchi[a,b], A. Solano[a,b], A. Staiano[a]

INFN Sezione di Trieste [a], Università di Trieste [b], Trieste, Italy
S. Belforte[a], V. Candelise[a,b,2], M. Casarsa[a], F. Cossutti[a], G. Della Ricca[a,b], B. Gobbo[a], C. La Licata[a,b], M. Marone[a,b], A. Schizzi[a,b], T. Umer[a,b], A. Zanetti[a]

Kangwon National University, Chunchon, Korea
S. Chang, A. Kropivnitskaya, S.K. Nam

Kyungpook National University, Daegu, Korea
D.H. Kim, G.N. Kim, M.S. Kim, D.J. Kong, S. Lee, Y.D. Oh, A. Sakharov, D.C. Son

Chonbuk National University, Jeonju, Korea
J.A. Brochero Cifuentes, H. Kim, T.J. Kim, M.S. Ryu

Chonnam National University, Institute for Universe and Elementary Particles, Kwangju, Korea
S. Song

Korea University, Seoul, Korea
S. Choi, Y. Go, D. Gyun, B. Hong, M. Jo, H. Kim, Y. Kim, B. Lee, K. Lee, K.S. Lee, S. Lee, S.K. Park, Y. Roh

Seoul National University, Seoul, Korea
H.D. Yoo

University of Seoul, Seoul, Korea
M. Choi, H. Kim, J.H. Kim, J.S.H. Lee, I.C. Park, G. Ryu

Sungkyunkwan University, Suwon, Korea
Y. Choi, Y.K. Choi, J. Goh, D. Kim, E. Kwon, J. Lee, I. Yu

Vilnius University, Vilnius, Lithuania
A. Juodagalvis, J. Vaitkus

National Centre for Particle Physics, Universiti Malaya, Kuala Lumpur, Malaysia
I. Ahmed, Z.A. Ibrahim, J.R. Komaragiri, M.A.B. Md Ali[32], F. Mohamad Idris[33], W.A.T. Wan Abdullah

Centro de Investigacion y de Estudios Avanzados del IPN, Mexico City, Mexico
E. Casimiro Linares, H. Castilla-Valdez, E. De La Cruz-Burelo, I. Heredia-de La Cruz[34], A. Hernandez-Almada, R. Lopez-Fernandez, A. Sanchez-Hernandez

Universidad Iberoamericana, Mexico City, Mexico
S. Carrillo Moreno, F. Vazquez Valencia

Benemerita Universidad Autonoma de Puebla, Puebla, Mexico
S. Carpinteyro, I. Pedraza, H.A. Salazar Ibarguen

Universidad Autónoma de San Luis Potosí, San Luis Potosí, Mexico
A. Morelos Pineda

University of Auckland, Auckland, New Zealand
D. Krofcheck

University of Canterbury, Christchurch, New Zealand
P.H. Butler, S. Reucroft

National Centre for Physics, Quaid-I-Azam University, Islamabad, Pakistan
A. Ahmad, M. Ahmad, Q. Hassan, H.R. Hoorani, W.A. Khan, T. Khurshid, M. Shoaib

National Centre for Nuclear Research, Swierk, Poland
H. Bialkowska, M. Bluj, B. Boimska, T. Frueboes, M. Górski, M. Kazana, K. Nawrocki, K. Romanowska-Rybinska, M. Szleper, P. Zalewski

Institute of Experimental Physics, Faculty of Physics, University of Warsaw, Warsaw, Poland
G. Brona, K. Bunkowski, K. Doroba, A. Kalinowski, M. Konecki, J. Krolikowski, M. Misiura, M. Olszewski, M. Walczak

Laboratório de Instrumentação e Física Experimental de Partículas, Lisboa, Portugal
P. Bargassa, C. Beirão Da Cruz E Silva, A. Di Francesco, P. Faccioli, P.G. Ferreira Parracho, M. Gallinaro, L. Lloret Iglesias, F. Nguyen, J. Rodrigues Antunes, J. Seixas, O. Toldaiev, D. Vadruccio, J. Varela, P. Vischia

Joint Institute for Nuclear Research, Dubna, Russia
S. Afanasiev, P. Bunin, M. Gavrilenko, I. Golutvin, I. Gorbunov, A. Kamenev, V. Karjavin, V. Konoplyanikov, A. Lanev, A. Malakhov, V. Matveev[35], P. Moisenz, V. Palichik, V. Perelygin, S. Shmatov, S. Shulha, N. Skatchkov, V. Smirnov, A. Zarubin

Petersburg Nuclear Physics Institute, Gatchina (St. Petersburg), Russia
V. Golovtsov, Y. Ivanov, V. Kim[36], E. Kuznetsova, P. Levchenko, V. Murzin, V. Oreshkin, I. Smirnov, V. Sulimov, L. Uvarov, S. Vavilov, A. Vorobyev

Institute for Nuclear Research, Moscow, Russia
Yu. Andreev, A. Dermenev, S. Gninenko, N. Golubev, A. Karneyeu, M. Kirsanov, N. Krasnikov, A. Pashenkov, D. Tlisov, A. Toropin

Institute for Theoretical and Experimental Physics, Moscow, Russia
V. Epshteyn, V. Gavrilov, N. Lychkovskaya, V. Popov, I. Pozdnyakov, G. Safronov, A. Spiridonov, E. Vlasov, A. Zhokin

National Research Nuclear University 'Moscow Engineering Physics Institute' (MEPhI), Moscow, Russia
A. Bylinkin

P.N. Lebedev Physical Institute, Moscow, Russia
V. Andreev, M. Azarkin[37], I. Dremin[37], M. Kirakosyan, A. Leonidov[37], G. Mesyats, S.V. Rusakov, A. Vinogradov

Skobeltsyn Institute of Nuclear Physics, Lomonosov Moscow State University, Moscow, Russia
A. Baskakov, A. Belyaev, E. Boos, M. Dubinin[38], L. Dudko, A. Ershov, A. Gribushin, V. Klyukhin, O. Kodolova, I. Lokhtin, I. Myagkov, S. Obraztsov, S. Petrushanko, V. Savrin, A. Snigirev

State Research Center of Russian Federation, Institute for High Energy Physics, Protvino, Russia
I. Azhgirey, I. Bayshev, S. Bitioukov, V. Kachanov, A. Kalinin, D. Konstantinov, V. Krychkine, V. Petrov, R. Ryutin, A. Sobol, L. Tourtchanovitch, S. Troshin, N. Tyurin, A. Uzunian, A. Volkov

University of Belgrade, Faculty of Physics and Vinca Institute of Nuclear Sciences, Belgrade, Serbia
P. Adzic[39], M. Ekmedzic, J. Milosevic, V. Rekovic

Centro de Investigaciones Energéticas Medioambientales y Tecnológicas (CIEMAT), Madrid, Spain
J. Alcaraz Maestre, E. Calvo, M. Cerrada, M. Chamizo Llatas, N. Colino, B. De La Cruz, A. Delgado Peris, D. Domínguez Vázquez, A. Escalante Del Valle, C. Fernandez Bedoya, J.P. Fernández Ramos, J. Flix, M.C. Fouz, P. Garcia-Abia, O. Gonzalez Lopez, S. Goy Lopez, J.M. Hernandez, M.I. Josa, E. Navarro De Martino, A. Pérez-Calero Yzquierdo, J. Puerta Pelayo, A. Quintario Olmeda, I. Redondo, L. Romero, M.S. Soares

Universidad Autónoma de Madrid, Madrid, Spain
C. Albajar, J.F. de Trocóniz, M. Missiroli, D. Moran

Universidad de Oviedo, Oviedo, Spain
H. Brun, J. Cuevas, J. Fernandez Menendez, S. Folgueras, I. Gonzalez Caballero, E. Palencia Cortezon, J.M. Vizan Garcia

Instituto de Física de Cantabria (IFCA), CSIC-Universidad de Cantabria, Santander, Spain
I.J. Cabrillo, A. Calderon, J.R. Castiñeiras De Saa, P. De Castro Manzano, J. Duarte Campderros, M. Fernandez, G. Gomez, A. Graziano, A. Lopez Virto, J. Marco, R. Marco, C. Martinez Rivero, F. Matorras, F.J. Munoz Sanchez, J. Piedra Gomez, T. Rodrigo, A.Y. Rodríguez-Marrero, A. Ruiz-Jimeno, L. Scodellaro, I. Vila, R. Vilar Cortabitarte

CERN, European Organization for Nuclear Research, Geneva, Switzerland
D. Abbaneo, E. Auffray, G. Auzinger, M. Bachtis, P. Baillon, A.H. Ball, D. Barney, A. Benaglia, J. Bendavid, L. Benhabib, J.F. Benitez, G.M. Berruti, G. Bianchi, P. Bloch, A. Bocci, A. Bonato, C. Botta, H. Breuker, T. Camporesi, G. Cerminara, S. Colafranceschi[40], M. D'Alfonso, D. d'Enterria, A. Dabrowski, V. Daponte, A. David, M. De Gruttola, F. De Guio, A. De Roeck, S. De Visscher, E. Di Marco, M. Dobson, M. Dordevic, T. du Pree, N. Dupont, A. Elliott-Peisert, J. Eugster, G. Franzoni, W. Funk, D. Gigi, K. Gill, D. Giordano, M. Girone, F. Glege, R. Guida, S. Gundacker, M. Guthoff, J. Hammer, M. Hansen, P. Harris, J. Hegeman, V. Innocente, P. Janot, H. Kirschenmann, M.J. Kortelainen, K. Kousouris, K. Krajczar, P. Lecoq, C. Lourenço, M.T. Lucchini, N. Magini, L. Malgeri, M. Mannelli, J. Marrouche, A. Martelli, L. Masetti, F. Meijers, S. Mersi, E. Meschi, F. Moortgat, S. Morovic, M. Mulders, M.V. Nemallapudi, H. Neugebauer, S. Orfanelli[41], L. Orsini, L. Pape, E. Perez, A. Petrilli, G. Petrucciani, A. Pfeiffer, D. Piparo, A. Racz, G. Rolandi[42], M. Rovere, M. Ruan, H. Sakulin, C. Schäfer, C. Schwick, A. Sharma, P. Silva, M. Simon, P. Sphicas[43], D. Spiga, J. Steggemann, B. Stieger, M. Stoye, Y. Takahashi, D. Treille, A. Tsirou, G.I. Veres[21], N. Wardle, H.K. Wöhri, A. Zagozdzinska[44], W.D. Zeuner

Paul Scherrer Institut, Villigen, Switzerland
W. Bertl, K. Deiters, W. Erdmann, R. Horisberger, Q. Ingram, H.C. Kaestli, D. Kotlinski, U. Langenegger, T. Rohe

Institute for Particle Physics, ETH Zurich, Zurich, Switzerland
F. Bachmair, L. Bäni, L. Bianchini, M.A. Buchmann, B. Casal, G. Dissertori, M. Dittmar, M. Donegà, M. Dünser, P. Eller, C. Grab, C. Heidegger, D. Hits, J. Hoss, G. Kasieczka, W. Lustermann, B. Mangano, A.C. Marini, M. Marionneau, P. Martinez Ruiz del Arbol, M. Masciovecchio, D. Meister, P. Musella, F. Nessi-Tedaldi, F. Pandolfi, J. Pata, F. Pauss, L. Perrozzi, M. Peruzzi, M. Quittnat, M. Rossini, A. Starodumov[45], M. Takahashi, V.R. Tavolaro, K. Theofilatos, R. Wallny, H.A. Weber

Universität Zürich, Zurich, Switzerland
T.K. Aarrestad, C. Amsler[46], L. Caminada, M.F. Canelli, V. Chiochia, A. De Cosa, C. Galloni, A. Hinzmann, T. Hreus, B. Kilminster, C. Lange, J. Ngadiuba, D. Pinna, P. Robmann, F.J. Ronga, D. Salerno, S. Taroni, Y. Yang

National Central University, Chung-Li, Taiwan
M. Cardaci, K.H. Chen, T.H. Doan, C. Ferro, M. Konyushikhin, C.M. Kuo, W. Lin, Y.J. Lu, R. Volpe, S.S. Yu

National Taiwan University (NTU), Taipei, Taiwan
R. Bartek, P. Chang, Y.H. Chang, Y.W. Chang, Y. Chao, K.F. Chen, P.H. Chen, C. Dietz, F. Fiori, U. Grundler, W.-S. Hou, Y. Hsiung, Y.F. Liu, R.-S. Lu, M. Miñano Moya, E. Petrakou, J.F. Tsai, Y.M. Tzeng

Chulalongkorn University, Faculty of Science, Department of Physics, Bangkok, Thailand
B. Asavapibhop, K. Kovitanggoon, G. Singh, N. Srimanobhas, N. Suwonjandee

Cukurova University, Adana, Turkey
A. Adiguzel, M.N. Bakirci[47], C. Dozen, I. Dumanoglu, E. Eskut, S. Girgis, G. Gokbulut, Y. Guler, E. Gurpinar, I. Hos, E.E. Kangal[48], G. Onengut[49], K. Ozdemir[50], S. Ozturk[47], A. Polatoz, D. Sunar Cerci[51], M. Vergili, C. Zorbilmez

Middle East Technical University, Physics Department, Ankara, Turkey
I.V. Akin, B. Bilin, S. Bilmis, B. Isildak[52], G. Karapinar[53], U.E. Surat, M. Yalvac, M. Zeyrek

Bogazici University, Istanbul, Turkey
E.A. Albayrak[54], E. Gülmez, M. Kaya[55], O. Kaya[56], T. Yetkin[57]

Istanbul Technical University, Istanbul, Turkey
K. Cankocak, S. Sen[58], F.I. Vardarlı

Institute for Scintillation Materials of National Academy of Science of Ukraine, Kharkov, Ukraine
B. Grynyov

National Scientific Center, Kharkov Institute of Physics and Technology, Kharkov, Ukraine
L. Levchuk, P. Sorokin

University of Bristol, Bristol, United Kingdom
R. Aggleton, F. Ball, L. Beck, J.J. Brooke, E. Clement, D. Cussans, H. Flacher, J. Goldstein, M. Grimes, G.P. Heath, H.F. Heath, J. Jacob, L. Kreczko, C. Lucas, Z. Meng, D.M. Newbold[59], S. Paramesvaran, A. Poll, T. Sakuma, S. Seif El Nasr-storey, S. Senkin, D. Smith, V.J. Smith

Rutherford Appleton Laboratory, Didcot, United Kingdom
K.W. Bell, A. Belyaev[60], C. Brew, R.M. Brown, D.J.A. Cockerill, J.A. Coughlan, K. Harder, S. Harper, E. Olaiya, D. Petyt, C.H. Shepherd-Themistocleous, A. Thea, L. Thomas, I.R. Tomalin, T. Williams, W.J. Womersley, S.D. Worm

Imperial College, London, United Kingdom
M. Baber, R. Bainbridge, O. Buchmuller, A. Bundock, D. Burton, S. Casasso, M. Citron, D. Colling, L. Corpe, N. Cripps, P. Dauncey, G. Davies, A. De Wit, M. Della Negra, P. Dunne, A. Elwood, W. Ferguson, J. Fulcher, D. Futyan, G. Hall, G. Iles, G. Karapostoli, M. Kenzie, R. Lane, R. Lucas[59], L. Lyons, A.-M. Magnan, S. Malik, J. Nash, A. Nikitenko[45], J. Pela, M. Pesaresi, K. Petridis, D.M. Raymond, A. Richards, A. Rose, C. Seez, A. Tapper, K. Uchida, M. Vazquez Acosta[61], T. Virdee, S.C. Zenz

Brunel University, Uxbridge, United Kingdom
J.E. Cole, P.R. Hobson, A. Khan, P. Kyberd, D. Leggat, D. Leslie, I.D. Reid, P. Symonds, L. Teodorescu, M. Turner

Baylor University, Waco, USA
A. Borzou, J. Dittmann, K. Hatakeyama, A. Kasmi, H. Liu, N. Pastika

The University of Alabama, Tuscaloosa, USA
O. Charaf, S.I. Cooper, C. Henderson, P. Rumerio

Boston University, Boston, USA
A. Avetisyan, T. Bose, C. Fantasia, D. Gastler, P. Lawson, D. Rankin, C. Richardson, J. Rohlf, J. St. John, L. Sulak, D. Zou

Brown University, Providence, USA
J. Alimena, E. Berry, S. Bhattacharya, D. Cutts, N. Dhingra, A. Ferapontov, A. Garabedian, U. Heintz, E. Laird, G. Landsberg, Z. Mao, M. Narain, S. Sagir, T. Sinthuprasith

University of California, Davis, Davis, USA
R. Breedon, G. Breto, M. Calderon De La Barca Sanchez, S. Chauhan, M. Chertok, J. Conway, R. Conway, P.T. Cox, R. Erbacher, M. Gardner, W. Ko, R. Lander, M. Mulhearn, D. Pellett, J. Pilot, F. Ricci-Tam, S. Shalhout, J. Smith, M. Squires, D. Stolp, M. Tripathi, S. Wilbur, R. Yohay

University of California, Los Angeles, USA
R. Cousins, P. Everaerts, C. Farrell, J. Hauser, M. Ignatenko, G. Rakness, D. Saltzberg, E. Takasugi, V. Valuev, M. Weber

University of California, Riverside, Riverside, USA
K. Burt, R. Clare, J. Ellison, J.W. Gary, G. Hanson, J. Heilman, M. Ivova PANEVA, P. Jandir, E. Kennedy, F. Lacroix, O.R. Long, A. Luthra, M. Malberti, M. Olmedo Negrete, A. Shrinivas, H. Wei, S. Wimpenny

University of California, San Diego, La Jolla, USA
J.G. Branson, G.B. Cerati, S. Cittolin, R.T. D'Agnolo, A. Holzner, R. Kelley, D. Klein, J. Letts, I. Macneill, D. Olivito, S. Padhi, M. Pieri, M. Sani, V. Sharma, S. Simon, M. Tadel, Y. Tu, A. Vartak, S. Wasserbaech[62], C. Welke, F. Würthwein, A. Yagil, G. Zevi Della Porta

University of California, Santa Barbara, Santa Barbara, USA
D. Barge, J. Bradmiller-Feld, C. Campagnari, A. Dishaw, V. Dutta, K. Flowers, M. Franco Sevilla, P. Geffert, C. George, F. Golf, L. Gouskos, J. Gran, J. Incandela, C. Justus, N. Mccoll, S.D. Mullin, J. Richman, D. Stuart, I. Suarez, W. To, C. West, J. Yoo

California Institute of Technology, Pasadena, USA
D. Anderson, A. Apresyan, A. Bornheim, J. Bunn, Y. Chen, J. Duarte, A. Mott, H.B. Newman, C. Pena, M. Pierini, M. Spiropulu, J.R. Vlimant, S. Xie, R.Y. Zhu

Carnegie Mellon University, Pittsburgh, USA
V. Azzolini, A. Calamba, B. Carlson, T. Ferguson, Y. Iiyama, M. Paulini, J. Russ, M. Sun, H. Vogel, I. Vorobiev

University of Colorado Boulder, Boulder, USA
J.P. Cumalat, W.T. Ford, A. Gaz, F. Jensen, A. Johnson, M. Krohn, T. Mulholland, U. Nauenberg, J.G. Smith, K. Stenson, S.R. Wagner

Cornell University, Ithaca, USA
J. Alexander, A. Chatterjee, J. Chaves, J. Chu, S. Dittmer, N. Eggert, N. Mirman, G. Nicolas Kaufman, J.R. Patterson, A. Rinkevicius, A. Ryd, L. Skinnari, L. Soffi, W. Sun, S.M. Tan, W.D. Teo, J. Thom, J. Thompson, J. Tucker, Y. Weng, P. Wittich

Fermi National Accelerator Laboratory, Batavia, USA
S. Abdullin, M. Albrow, J. Anderson, G. Apollinari, L.A.T. Bauerdick, A. Beretvas, J. Berryhill, P.C. Bhat, G. Bolla, K. Burkett, J.N. Butler, H.W.K. Cheung, F. Chlebana, S. Cihangir, V.D. Elvira, I. Fisk, J. Freeman, E. Gottschalk, L. Gray, D. Green, S. Grünendahl, O. Gutsche, J. Hanlon, D. Hare, R.M. Harris, J. Hirschauer, B. Hooberman, Z. Hu, S. Jindariani, M. Johnson, U. Joshi, A.W. Jung, B. Klima, B. Kreis, S. Kwan[†], S. Lammel, J. Linacre, D. Lincoln, R. Lipton, T. Liu, R. Lopes De Sá, J. Lykken, K. Maeshima, J.M. Marraffino, V.I. Martinez Outschoorn, S. Maruyama, D. Mason, P. McBride, P. Merkel, K. Mishra, S. Mrenna, S. Nahn, C. Newman-Holmes, V. O'Dell, O. Prokofyev, E. Sexton-Kennedy, A. Soha, W.J. Spalding, L. Spiegel,

L. Taylor, S. Tkaczyk, N.V. Tran, L. Uplegger, E.W. Vaandering, C. Vernieri, M. Verzocchi, R. Vidal, A. Whitbeck, F. Yang, H. Yin

University of Florida, Gainesville, USA
D. Acosta, P. Avery, P. Bortignon, D. Bourilkov, A. Carnes, M. Carver, D. Curry, S. Das, G.P. Di Giovanni, R.D. Field, M. Fisher, I.K. Furic, J. Hugon, J. Konigsberg, A. Korytov, J.F. Low, P. Ma, K. Matchev, H. Mei, P. Milenovic[63], G. Mitselmakher, L. Muniz, D. Rank, R. Rossin, L. Shchutska, M. Snowball, D. Sperka, J. Wang, S. Wang, J. Yelton

Florida International University, Miami, USA
S. Hewamanage, S. Linn, P. Markowitz, G. Martinez, J.L. Rodriguez

Florida State University, Tallahassee, USA
A. Ackert, J.R. Adams, T. Adams, A. Askew, J. Bochenek, B. Diamond, J. Haas, S. Hagopian, V. Hagopian, K.F. Johnson, A. Khatiwada, H. Prosper, V. Veeraraghavan, M. Weinberg

Florida Institute of Technology, Melbourne, USA
V. Bhopatkar, M. Hohlmann, H. Kalakhety, D. Mareskas-palcek, T. Roy, F. Yumiceva

University of Illinois at Chicago (UIC), Chicago, USA
M.R. Adams, L. Apanasevich, D. Berry, R.R. Betts, I. Bucinskaite, R. Cavanaugh, O. Evdokimov, L. Gauthier, C.E. Gerber, D.J. Hofman, P. Kurt, C. O'Brien, I.D. Sandoval Gonzalez, C. Silkworth, P. Turner, N. Varelas, Z. Wu, M. Zakaria

The University of Iowa, Iowa City, USA
B. Bilki[64], W. Clarida, K. Dilsiz, S. Durgut, R.P. Gandrajula, M. Haytmyradov, V. Khristenko, J.-P. Merlo, H. Mermerkaya[65], A. Mestvirishvili, A. Moeller, J. Nachtman, H. Ogul, Y. Onel, F. Ozok[54], A. Penzo, C. Snyder, P. Tan, E. Tiras, J. Wetzel, K. Yi

Johns Hopkins University, Baltimore, USA
I. Anderson, B.A. Barnett, B. Blumenfeld, D. Fehling, L. Feng, A.V. Gritsan, P. Maksimovic, C. Martin, K. Nash, M. Osherson, M. Swartz, M. Xiao, Y. Xin

The University of Kansas, Lawrence, USA
P. Baringer, A. Bean, G. Benelli, C. Bruner, J. Gray, R.P. Kenny III, D. Majumder, M. Malek, M. Murray, D. Noonan, S. Sanders, R. Stringer, Q. Wang, J.S. Wood

Kansas State University, Manhattan, USA
I. Chakaberia, A. Ivanov, K. Kaadze, S. Khalil, M. Makouski, Y. Maravin, L.K. Saini, N. Skhirtladze, I. Svintradze, S. Toda

Lawrence Livermore National Laboratory, Livermore, USA
D. Lange, F. Rebassoo, D. Wright

University of Maryland, College Park, USA
C. Anelli, A. Baden, O. Baron, A. Belloni, B. Calvert, S.C. Eno, C. Ferraioli, J.A. Gomez, N.J. Hadley, S. Jabeen, R.G. Kellogg, T. Kolberg, J. Kunkle, Y. Lu, A.C. Mignerey, K. Pedro, Y.H. Shin, A. Skuja, M.B. Tonjes, S.C. Tonwar

Massachusetts Institute of Technology, Cambridge, USA
A. Apyan, R. Barbieri, A. Baty, K. Bierwagen, S. Brandt, W. Busza, I.A. Cali, Z. Demiragli, L. Di Matteo, G. Gomez Ceballos, M. Goncharov, D. Gulhan, G.M. Innocenti, M. Klute, D. Kovalskyi, Y.S. Lai, Y.-J. Lee, A. Levin, P.D. Luckey, C. Mcginn, X. Niu, C. Paus, D. Ralph, C. Roland, G. Roland, J. Salfeld-Nebgen, G.S.F. Stephans, K. Sumorok, M. Varma, D. Velicanu, J. Veverka, J. Wang, T.W. Wang, B. Wyslouch, M. Yang, V. Zhukova

University of Minnesota, Minneapolis, USA
B. Dahmes, A. Finkel, A. Gude, P. Hansen, S. Kalafut, S.C. Kao, K. Klapoetke, Y. Kubota, Z. Lesko, J. Mans, S. Nourbakhsh, N. Ruckstuhl, R. Rusack, N. Tambe, J. Turkewitz

University of Mississippi, Oxford, USA
J.G. Acosta, S. Oliveros

University of Nebraska-Lincoln, Lincoln, USA
E. Avdeeva, K. Bloom, S. Bose, D.R. Claes, A. Dominguez, C. Fangmeier, R. Gonzalez Suarez, R. Kamalieddin, J. Keller, D. Knowlton, I. Kravchenko, J. Lazo-Flores, F. Meier, J. Monroy, F. Ratnikov, J.E. Siado, G.R. Snow

State University of New York at Buffalo, Buffalo, USA
M. Alyari, J. Dolen, J. George, A. Godshalk, I. Iashvili, J. Kaisen, A. Kharchilava, A. Kumar, S. Rappoccio

Northeastern University, Boston, USA
G. Alverson, E. Barberis, D. Baumgartel, M. Chasco, A. Hortiangtham, A. Massironi, D.M. Morse, D. Nash, T. Orimoto, R. Teixeira De Lima, D. Trocino, R.-J. Wang, D. Wood, J. Zhang

Northwestern University, Evanston, USA
K.A. Hahn, A. Kubik, N. Mucia, N. Odell, B. Pollack, A. Pozdnyakov, M. Schmitt, S. Stoynev, K. Sung, M. Trovato, M. Velasco, S. Won

University of Notre Dame, Notre Dame, USA
A. Brinkerhoff, N. Dev, M. Hildreth, C. Jessop, D.J. Karmgard, N. Kellams, K. Lannon, S. Lynch, N. Marinelli, F. Meng, C. Mueller, Y. Musienko[35], T. Pearson, M. Planer, R. Ruchti, G. Smith, N. Valls, M. Wayne, M. Wolf, A. Woodard

The Ohio State University, Columbus, USA
L. Antonelli, J. Brinson, B. Bylsma, L.S. Durkin, S. Flowers, A. Hart, C. Hill, R. Hughes, K. Kotov, T.Y. Ling, B. Liu, W. Luo, D. Puigh, M. Rodenburg, B.L. Winer, H.W. Wulsin

Princeton University, Princeton, USA
O. Driga, P. Elmer, J. Hardenbrook, P. Hebda, S.A. Koay, P. Lujan, D. Marlow, T. Medvedeva, M. Mooney, J. Olsen, C. Palmer, P. Piroué, X. Quan, H. Saka, D. Stickland, C. Tully, J.S. Werner, A. Zuranski

University of Puerto Rico, Mayaguez, USA
S. Malik

Purdue University, West Lafayette, USA
V.E. Barnes, D. Benedetti, D. Bortoletto, L. Gutay, M.K. Jha, M. Jones, K. Jung, M. Kress, N. Leonardo, D.H. Miller, N. Neumeister, F. Primavera, B.C. Radburn-Smith, X. Shi, I. Shipsey, D. Silvers, J. Sun, A. Svyatkovskiy, F. Wang, W. Xie, L. Xu, J. Zablocki

Purdue University Calumet, Hammond, USA
N. Parashar, J. Stupak

Rice University, Houston, USA
A. Adair, B. Akgun, Z. Chen, K.M. Ecklund, F.J.M. Geurts, M. Guilbaud, W. Li, B. Michlin, M. Northup, B.P. Padley, R. Redjimi, J. Roberts, J. Rorie, Z. Tu, J. Zabel

University of Rochester, Rochester, USA
B. Betchart, A. Bodek, P. de Barbaro, R. Demina, Y. Eshaq, T. Ferbel, M. Galanti, A. Garcia-Bellido, P. Goldenzweig, J. Han, A. Harel, O. Hindrichs, A. Khukhunaishvili, G. Petrillo, M. Verzetti

The Rockefeller University, New York, USA
L. Demortier

Rutgers, The State University of New Jersey, Piscataway, USA
S. Arora, A. Barker, J.P. Chou, C. Contreras-Campana, E. Contreras-Campana, D. Duggan, D. Ferencek, Y. Gershtein, R. Gray, E. Halkiadakis, D. Hidas, E. Hughes, S. Kaplan, R. Kunnawalkam Elayavalli, A. Lath, S. Panwalkar, M. Park, S. Salur, S. Schnetzer, D. Sheffield, S. Somalwar, R. Stone, S. Thomas, P. Thomassen, M. Walker

University of Tennessee, Knoxville, USA
M. Foerster, G. Riley, K. Rose, S. Spanier, A. York

Texas A&M University, College Station, USA
O. Bouhali[66], A. Castaneda Hernandez, M. Dalchenko, M. De Mattia, A. Delgado, S. Dildick, R. Eusebi, W. Flanagan, J. Gilmore, T. Kamon[67], V. Krutelyov, R. Montalvo, R. Mueller, I. Osipenkov, Y. Pakhotin, R. Patel, A. Perloff, J. Roe, A. Rose, A. Safonov, A. Tatarinov, K.A. Ulmer[2]

Texas Tech University, Lubbock, USA
N. Akchurin, C. Cowden, J. Damgov, C. Dragoiu, P.R. Dudero, J. Faulkner, S. Kunori, K. Lamichhane, S.W. Lee, T. Libeiro, S. Undleeb, I. Volobouev

Vanderbilt University, Nashville, USA
E. Appelt, A.G. Delannoy, S. Greene, A. Gurrola, R. Janjam, W. Johns, C. Maguire, Y. Mao, A. Melo, P. Sheldon, B. Snook, S. Tuo, J. Velkovska, Q. Xu

University of Virginia, Charlottesville, USA
M.W. Arenton, S. Boutle, B. Cox, B. Francis, J. Goodell, R. Hirosky, A. Ledovskoy, H. Li, C. Lin, C. Neu, E. Wolfe, J. Wood, F. Xia

Wayne State University, Detroit, USA
C. Clarke, R. Harr, P.E. Karchin, C. Kottachchi Kankanamge Don, P. Lamichhane, J. Sturdy

University of Wisconsin, Madison, USA
D.A. Belknap, D. Carlsmith, M. Cepeda, A. Christian, S. Dasu, L. Dodd, S. Duric, E. Friis, B. Gomber, M. Grothe, R. Hall-Wilton, M. Herndon, A. Hervé, P. Klabbers, A. Lanaro, A. Levine, K. Long, R. Loveless, A. Mohapatra, I. Ojalvo, T. Perry, G.A. Pierro, G. Polese, I. Ross, T. Ruggles, T. Sarangi, A. Savin, A. Sharma, N. Smith, W.H. Smith, D. Taylor, N. Woods

†: Deceased
1: Also at Vienna University of Technology, Vienna, Austria
2: Also at CERN, European Organization for Nuclear Research, Geneva, Switzerland
3: Also at State Key Laboratory of Nuclear Physics and Technology, Peking University, Beijing, China
4: Also at Institut Pluridisciplinaire Hubert Curien, Université de Strasbourg, Université de Haute Alsace Mulhouse, CNRS/IN2P3, Strasbourg, France
5: Also at National Institute of Chemical Physics and Biophysics, Tallinn, Estonia
6: Also at Skobeltsyn Institute of Nuclear Physics, Lomonosov Moscow State University, Moscow, Russia

7: Also at Universidade Estadual de Campinas, Campinas, Brazil
8: Also at Centre National de la Recherche Scientifique (CNRS) - IN2P3, Paris, France
9: Also at Laboratoire Leprince-Ringuet, Ecole Polytechnique, IN2P3-CNRS, Palaiseau, France
10: Also at Joint Institute for Nuclear Research, Dubna, Russia
11: Now at Helwan University, Cairo, Egypt
12: Also at Suez University, Suez, Egypt
13: Also at British University in Egypt, Cairo, Egypt
14: Also at Cairo University, Cairo, Egypt
15: Now at Fayoum University, El-Fayoum, Egypt
16: Now at Ain Shams University, Cairo, Egypt
17: Also at Université de Haute Alsace, Mulhouse, France
18: Also at Tbilisi State University, Tbilisi, Georgia
19: Also at Brandenburg University of Technology, Cottbus, Germany
20: Also at Institute of Nuclear Research ATOMKI, Debrecen, Hungary
21: Also at Eötvös Loránd University, Budapest, Hungary
22: Also at University of Debrecen, Debrecen, Hungary
23: Also at Wigner Research Centre for Physics, Budapest, Hungary
24: Also at University of Visva-Bharati, Santiniketan, India
25: Now at King Abdulaziz University, Jeddah, Saudi Arabia
26: Also at University of Ruhuna, Matara, Sri Lanka
27: Also at Isfahan University of Technology, Isfahan, Iran
28: Also at University of Tehran, Department of Engineering Science, Tehran, Iran
29: Also at Plasma Physics Research Center, Science and Research Branch, Islamic Azad University, Tehran, Iran
30: Also at Università degli Studi di Siena, Siena, Italy
31: Also at Purdue University, West Lafayette, USA
32: Also at International Islamic University of Malaysia, Kuala Lumpur, Malaysia
33: Also at Malaysian Nuclear Agency, MOSTI, Kajang, Malaysia
34: Also at Consejo Nacional de Ciencia y Tecnología, Mexico city, Mexico
35: Also at Institute for Nuclear Research, Moscow, Russia
36: Also at St. Petersburg State Polytechnical University, St. Petersburg, Russia
37: Also at National Research Nuclear University 'Moscow Engineering Physics Institute' (MEPhI), Moscow, Russia
38: Also at California Institute of Technology, Pasadena, USA
39: Also at Faculty of Physics, University of Belgrade, Belgrade, Serbia
40: Also at Facoltà Ingegneria, Università di Roma, Roma, Italy
41: Also at National Technical University of Athens, Athens, Greece
42: Also at Scuola Normale e Sezione dell'INFN, Pisa, Italy
43: Also at University of Athens, Athens, Greece
44: Also at Warsaw University of Technology, Institute of Electronic Systems, Warsaw, Poland
45: Also at Institute for Theoretical and Experimental Physics, Moscow, Russia
46: Also at Albert Einstein Center for Fundamental Physics, Bern, Switzerland
47: Also at Gaziosmanpasa University, Tokat, Turkey
48: Also at Mersin University, Mersin, Turkey
49: Also at Cag University, Mersin, Turkey
50: Also at Piri Reis University, Istanbul, Turkey
51: Also at Adiyaman University, Adiyaman, Turkey
52: Also at Ozyegin University, Istanbul, Turkey
53: Also at Izmir Institute of Technology, Izmir, Turkey

54: Also at Mimar Sinan University, Istanbul, Istanbul, Turkey
55: Also at Marmara University, Istanbul, Turkey
56: Also at Kafkas University, Kars, Turkey
57: Also at Yildiz Technical University, Istanbul, Turkey
58: Also at Hacettepe University, Ankara, Turkey
59: Also at Rutherford Appleton Laboratory, Didcot, United Kingdom
60: Also at School of Physics and Astronomy, University of Southampton, Southampton, United Kingdom
61: Also at Instituto de Astrofísica de Canarias, La Laguna, Spain
62: Also at Utah Valley University, Orem, USA
63: Also at University of Belgrade, Faculty of Physics and Vinca Institute of Nuclear Sciences, Belgrade, Serbia
64: Also at Argonne National Laboratory, Argonne, USA
65: Also at Erzincan University, Erzincan, Turkey
66: Also at Texas A&M University at Qatar, Doha, Qatar
67: Also at Kyungpook National University, Daegu, Korea